Counting trees in supersymmetric quantum mechanics

Clay Córdova and Shu-Heng Shao

Abstract. We study the supersymmetric ground states of the Kronecker model of quiver quantum mechanics. This is the simplest quiver with two gauge groups and bifundamental matter fields, and appears universally in four-dimensional $\mathcal{N} = 2$ systems. The ground state degeneracy may be written as a multi-dimensional contour integral, and the enumeration of poles can be simply phrased as counting bipartite trees. We solve this combinatorics problem, thereby obtaining exact formulas for the degeneracies of an infinite class of models. We also develop an algorithm to compute the angular momentum of the ground states, and present explicit expressions for the refined indices of theories where one rank is small.

Contents

1. Introduction

One of the most basic problems in any quantum system is to determine the spectrum of stable states. However, outside the realm of perturbation theory and exactly solvable models the answer to this question is elusive. One class of examples where progress is possible are those enjoying supersymmetry. In general, these models are not exactly solvable, yet nevertheless there are states in the spectrum whose existence and properties can be reliably determined. These supersymmetric models yield a window into non-perturbative physics where strong coupling phenomena may be confronted analytically. In particular, field theories and gravities with extended supersymmetry provide a class of models where exact spectroscopy results are feasible.

Motivated by these general considerations, in this work we analyze in detail a non-trivial model of supersymmetric particle spectroscopy. We consider a non-relativistic quantum mechanical system with two distinct species of (super)particles, and four supercharges. Each particle carries minimal angular momentum, and electromagnetic charges γ_1 and γ_2. The low-energy interactions of the system are invariantly characterized by the integral Dirac pairing of the electromagnetic charges

$$\langle \gamma_1, \gamma_2 \rangle = k > 0. \tag{1.1}$$

Our aim is to determine the non-relativistic bound state spectrum formed by M particles of type one, and N particles of type two. The system and its interactions are encoded in a quiver diagram, known as the *Kronecker* quiver shown below.[1]
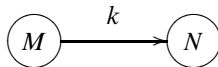
Figure 1. The Kronecker quiver with dimension vector (M, N) and k arrows. The quiver encodes the interaction of M particles of charge γ_1 and N particles of charge γ_2 with $\langle \gamma_1, \gamma_2 \rangle = k$.

We study only those bound states which preserve all four supercharges. These are the supersymmetric ground states of this quiver quantum mechanics. We denote their degeneracy by $\Omega(M, N, k)$. The Kronecker quiver model and the degeneracies $\Omega(M, N, k)$, have been previously studied from a variety of perspectives, including quantum groups [2], wall-crossing formulas [3–5], spectral networks [6, 7], and equivariant cohomology [8, 9].

---

[1] The explicit expression for the Hamiltonian of this system may be found, for instance, in [1].

Our main result, described in detail in §2 and §3, is a formula for $\Omega(M, N, k)$ in the special case where the parameter N may be expressed as $N = Mr + 1$ for r a non-negative integer. It is simplest to state our results in terms of a generating function. Introduce $F(k, r, x)$ which depends on a formal variable x as

$$F(k, r, x) = (k - r) \sum_{\ell=1}^{\infty} \frac{(-1)^{\ell-1}}{\ell} \binom{k\ell}{r\ell} x^{\ell}. \qquad (1.2)$$

and let $[x^j]\{q(x)\}$ denote the coefficient of x^j in a power series $q(x)$. Then, we find

$$\Omega(M, Mr + 1, k) = \frac{1}{(Mr + 1)^2} [x^M]\{\exp[(Mr + 1)F(k, r, x)]\}. \qquad (1.3)$$

In the further limit $r \to 1$, the generating function simplifies dramatically and we are able to provide a closed form expression

$$\Omega(M, M + 1, k) = \frac{k}{(M + 1)[(k - 1)M + k]} \binom{(k - 1)^2 M + k(k - 1)}{M}, \qquad (1.4)$$

thus reproducing the results of [8]. In §6, we also develop an algorithm to compute the angular momentum of the ground states, and apply our algorithm to ground states with small M and arbitrary N in equation (6.30).

The method that we use to derive (1.3) is supersymmetric localization [10–12]. This technique expresses the index $\Omega(M, N, k)$ as a multidimensional contour integral [13]. Our key technical results, proved in §4, are a systematic combinatorial interpretation of the residues of this integral. Specifically, we demonstrate that enumeration of poles in the contour integral is equivalent to counting certain bipartite trees. The computation of the number of such trees is an elementary problem in graph theory which we solve in §5. Its solution leads to the index formula (1.3).

The index formula that we obtain is also of interest in a purely mathematical context. As we review in §2, the index $\Omega(M, N, k)$ can be interpreted as the Euler characteristic of the moduli space $\mathcal{M}_{M,N}^k$ of stable representations of the Kronecker quiver. These Kronecker moduli spaces are a natural generalization of Grassmannians. Our combinatorial interpretation of the cohomology of $\mathcal{M}_{M,N}^k$ is thus reminiscent of classical results in Schubert calculus.

One virtue of the supersymmetric localization framework we employ is that the complexity of the quiver moduli spaces is bypassed. The desired Euler characteristics are expressed as integrals over an auxiliary parameter space (physically vector multiplet zero modes). Nevertheless we find that certain aspects of quiver representation theory appear in our calculation. Specifically, the problem of tree

counting that appears in our residue integral is very reminiscent of the combi-
natorics that emerges from equivariant localization directly on the quiver mod-
uli spaces [8].[2] Fleshing out the relationship between equivariant localization on
moduli space and the supersymmetric localization framework is an interesting di-
rection for future work.

Our results have broad applications in $\mathcal{N} = 2$ field theories and supergravity.
Indeed, in a wide class of such systems, the supersymmetric particles and black
holes may be captured by a non-relativistic quiver quantum mechanics [1,14–23].
The Kronecker model that we study, describes a subset of all such quiver quantum
mechanics systems: it encodes the bound states whose electromagnetic charges
lie in a sublattice spanned by two primitive charges (see, for example, Figure 2).
Moreover, the spectrum of this model illustrates universal physical features such
as Regge trajectories [24], and an exponential degeneracy of states [6,8,25,26].
Finally, the degeneracies $\Omega(M, N, k)$ are also interesting due to the distinguished
role that they play in wall-crossing formulas [3].

(a)   (b)   (c)
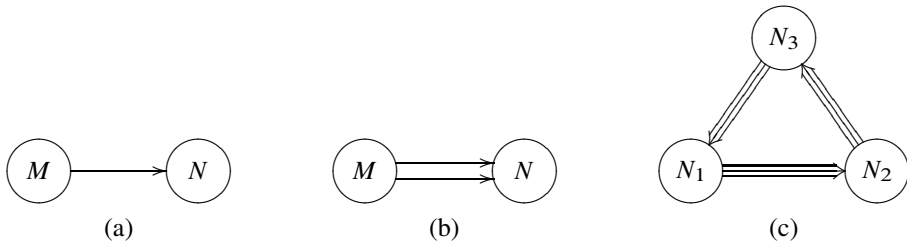
Figure 2. Examples of Kronecker quivers occur in many well-known models. The case
$k = 1$, illustrated in (a), describes the spectrum of the Argyres–Douglas conformal field
theory [27–29]. The case $k = 2$, illustrated in (b), describes the spectrum of SU(2) Seiberg-
Witten theory [17,30]. The case $k > 2$ occurs frequently as a subset of the bound states
in many $\mathcal{N} = 2$ systems. For instance, the $k = 3$ case in (c) appears in the quiver that
describes the bound states of D-branes in type IIA string theory on local $\mathbb{P}^2$ [15]. More
generally, all Kronecker quivers with $k > 2$ occur as subsectors of the quiver describing
bound states in SU(N) super-Yang–Mills [6].

There are a number of significant questions left unanswered by our analysis.
Most glaringly, it would be interesting to extend our result (1.3) to the general
value of parameters (M, N, k), and thereby provide a complete solution to the
Kronecker model. More conceptually, the exponential resummation appearing
in (1.3) is qualitatively similar to the general relationship between Donaldson–
Thomas invariants and Gromov–Witten invariants [31,32]. This suggests, perhaps,

---

[2] We thank the anonymous referee for pointing out this potential connection.

that the function $F(k, r, x)$ itself admits a direct enumerative meaning. Finally, it would be satisfying to explain the physical significance of the bipartite trees which play a crucial technical role in this work, perhaps by relating them to attractor flow trees [33, 34]. We leave these problems as potential avenues for future investigation.

2. Kronecker quivers

In this section, we give an overview of our main result for the degeneracies $\Omega(M, N, k)$. Complete proofs of all ingredients presented may be found in §4 and §5.

We begin in §2.1 with a review of the geometry underlying the indices of the Kronecker quiver, and explain how the degeneracies $\Omega(M, N, k)$ may be viewed as the Euler characteristic of the Kronecker moduli space. Next in §2.2 and §2.3 we overview the main steps in our calculation. In particular, we describe how counting bipartite trees is related to computing indices and in §2.3.1 we state a theorem which enables us to enumerate all such trees. Finally, in §2.4 we assemble the pieces into a formula for $\Omega(M, N, k)$, in the special case $N = Mr + 1$.

2.1. Kronecker moduli and the index. In any model of quiver quantum mechanics with four supercharges, the problem of determining the ground state spectrum can be phrased in a completely geometric language in terms of quiver moduli spaces. In this section we review this connection in the context of the Kronecker quiver.

Consider the Kronecker quiver illustrated in Figure 1. The Lagrangian for this system is a gauged $\mathcal{N} = 4$ quantum mechanics. Each node supports a unitary gauge group of ranks M and N respectively with associated vector multiplets, while the arrows of the quiver are bifundamental chiral multiplet matter fields. The explicit expression for the Hamiltonian of this system may be found, for instance, in [1].

The system has a classical Higgs branch moduli space $\mathcal{M}_{M,N}^k$ described in a standard way. The chiral multiplet fields Φ_i ($i = 1, \ldots, k$) have constant expectation values. Thus, they may be viewed as specifying linear maps

$$\Phi_i \colon \mathbb{C}^M \longrightarrow \mathbb{C}^N. \tag{2.1}$$

On the set of possible field expectation values we impose the D-term equations

$$\sum_{i=1}^{k} \Phi_i^\dagger \circ \Phi_i = \zeta I_M, \quad \sum_{i=1}^{k} \Phi_i \circ \Phi_i^\dagger = \frac{M\zeta}{N} I_N, \tag{2.2}$$

where in the above, $\zeta > 0$ is the Fayet–Iliopoulos parameter,[3] and I_L is the $L \times L$ identity matrix. Finally, the locus of solutions to the D-term equation (2.2) is invariant under the action of the gauge group $U(M) \times U(N)$ acting on the Φ_i via the bifundamental representation. The desired moduli space $\mathcal{M}_{M,N}^k$ is the quotient space

$$\mathcal{M}_{M,N}^k \equiv \left\{ \Phi_i \; \middle| \; \sum_{i=1}^{k} \Phi_i^\dagger \circ \Phi_i = \zeta I_M, \; \sum_{i=1}^{k} \Phi_i \circ \Phi_i^\dagger = \frac{M\zeta}{N} I_N \right\} / U(M) \times U(N). \tag{2.3}$$

For a discussion of these moduli spaces from the mathematical point of view see e.g. [35].

The Kronecker moduli spaces $\mathcal{M}_{M,N}^k$ have several features which follow directly from their construction as quotients, as well as through the application of Seiberg dualities (quiver mutations [36, 37]). We state these facts here. Throughout this discussion, we assume that the pair (M, N) is coprime, to avoid various subtleties.

- The moduli space $\mathcal{M}_{M,N}^k$ is a smooth compact Kähler manifold (if it is non-empty), with metric inherited via its construction as a Kähler quotient.

- The complex dimension of $\mathcal{M}_{M,N}^k$ is

$$\dim(\mathcal{M}_{M,N}^k) = kNM - M^2 - N^2 + 1. \tag{2.4}$$

  In particular, the moduli space is non-empty if and only if the above dimension formula is non-negative.

- In the Hodge decomposition of the cohomology of $\mathcal{M}_{M,N}^k$, we have the following vanishing theorem: [2]

$$p \neq q \implies h^{p,q}(\mathcal{M}_{M,N}^k) = 0. \tag{2.5}$$

- We have the following isomorphisms [36, 37]:

$$\begin{aligned} \text{Reflection:} \quad & \mathcal{M}_{M,N}^k \cong \mathcal{M}_{N,M}^k, \\ \text{Mutation:} \quad & \mathcal{M}_{M,N}^k \cong \mathcal{M}_{N,Nk-M}^k. \end{aligned} \tag{2.6}$$

[3] When $\zeta < 0$ all moduli spaces are empty, illustrating the wall-crossing phenomenon.

According to familiar results in supersymmetric quantum mechanics, the supersymmetric ground states may be extracted from the cohomology of the moduli space. Moreover, the data of the spin of ground states (an SU(2) representation) is determined by the Lefschetz SU(2) action on the cohomology.

Complete information about the ground state spectrum is conveniently packaged into a refined index depending on a fugacity y which encodes the angular momentum

$$\Omega(M, N, k, y) \equiv \sum_{p=0}^{d} y^{2p-d} \, h^{p,p}(\mathcal{M}_{M,N}^k), \tag{2.7}$$

where in the above, d denotes the complex dimension of the moduli space given in (2.4). Up to the overall factor of y^{-d}, this index coincides with the Hirzebruch χ_y genus. In particular, in the specialization $y \to 1$ the above reduces to the Euler characteristic

$$\Omega(M, N, k) \equiv \Omega(M, N, k, 1) = \sum_{p=0}^{d} h^{p,p}(\mathcal{M}_{M,N}^k) = \chi(\mathcal{M}_{M,N}^k). \tag{2.8}$$

One notable feature of both (2.7) and (2.8) is that the Betti numbers are weighted without signs. Thus, $\Omega(M, N, k, y)$, which a priori is an index and counts states up to signs, in fact computes the exact degeneracy due to the vanishing result (2.5) on the cohomology.[4]

The indices (2.8) and (2.7) are the quantities that we compute in this work. Our main results concern the Euler characteristic (2.8). In §6 we present an algorithm to determine the complete cohomology generating function (2.7).

2.1.1. The Grassmannian as a Kronecker moduli space. In this section we provide some intuition for Kronecker moduli spaces, by demonstrating that in the special case $(M, N) = (M, 1)$, the moduli space reduces to a Grassmannian.

To illustrate this isomorphism, we first write the maps Φ_i as a row vector

$$\Phi_i = \begin{pmatrix} \phi_i^1 & \phi_i^2 & \dots & \phi_i^M \end{pmatrix}. \tag{2.9}$$

The k distinct row vectors may then be assembled into a $k \times M$ matrix X as

$$X = \begin{pmatrix} \phi_1^1 & \phi_1^2 & \dots & \phi_1^M \\ \phi_2^1 & \phi_2^2 & \dots & \phi_2^M \\ \vdots & \vdots & \ddots & \vdots \\ \phi_k^1 & \phi_k^2 & \dots & \phi_k^M \end{pmatrix}. \tag{2.10}$$

---

[4] This is a special case of the "No-Exotics" conjecture [38, 39].

The D-term equation (2.2) asserts that the M columns of this matrix are pairwise orthogonal and that they each have norm ζ. From this we conclude that matrix X must have rank M and hence in particular the moduli space is empty if $M > k$.

On the other hand if $M \leq k$, then the columns of the matrix X comprise a unitary frame for an M-plane in $\mathbb{C}^k$. The gauge group $U(M)$ acts on X as $X \rightarrow XG$ and hence may be viewed as changing the unitary frame for the M-plane. We conclude that the moduli space is a Grassmannian

$$\mathcal{M}_{M,1}^k \cong \mathrm{Gr}(M, k). \tag{2.11}$$

The cohomology of the Grassmannian is well-known, and via (2.7) we are able to write the generating function

$$\Omega(M, 1, k, y) = \begin{cases} \dfrac{y^{M(M-k)} \prod_{i=1}^{k}(1 - y^{2i})}{\prod_{i=1}^{M}(1 - y^{2i}) \prod_{i=1}^{k-M}(1 - y^{2i})}, & k \geq M, \\ 0, & k < M. \end{cases} \tag{2.12}$$

In particular, evaluating at $y = 1$, we have

$$\Omega(M, 1, k) = \chi(\mathcal{M}_{M,1}^k) = \begin{cases} \dbinom{k}{M}, & k \geq M, \\ 0, & k < M. \end{cases} \tag{2.13}$$

This result serves two purposes. First, the explicit formulas (2.12)-(2.13) serve as useful grounding cases against which we can benchmark our more general results. Second, it provides some intuition about the nature of Kronecker moduli spaces. The Grassmannian $\mathrm{Gr}(M, k)$ describes vectors in generic position (enforced by the D-term equation (2.2)). The Kronecker moduli spaces $\mathcal{M}_{M,N}^k$ generalize this idea, and describe configurations of matrices in general position.

2.1.2. Moduli spaces as a function of k. Another way to gain intuition about Kronecker moduli spaces is to examine them as a function of the number of arrows k. Consider the special case [5] $M = N$. Then, the moduli space describes k linear maps

$$\Phi_i \colon \mathbb{C}^M \longrightarrow \mathbb{C}^M. \tag{2.14}$$

As a consequence of the D-term equation, these maps are in general position and hence, on an open set in the moduli space, at least one of them is invertible.

---

[5] Since the dimension vectors are not coprime, in this case one should consider the moduli of semi-stable representations as opposed to stable representations.

One may then fix some of the gauge redundancy by going to a basis where this invertible map is the identity.

What remains after this is $k - 1$ linear maps, where now the remaining gauge redundancy acts as conjugation. For $k = 1$ this problem is trivial. For $k = 2$, this problem is solved by the Jordan decomposition theorem. Correspondingly, for $k = 1, 2$ all Kronecker moduli spaces may be explicitly determined.

Finally, for $k > 2$ these moduli spaces parameterize multiple linear maps up to conjugation. This is a notoriously wild representation theory problem, and there is no known general description of the moduli space $\mathcal{M}^k_{M,N}$. Despite the complexity for large k, we will be able to obtain simple exact formulas for the numerical invariants of these moduli spaces.

2.2. The degeneration formula and star quivers. In order to determine a formula for the Euler characteristic of Kronecker moduli space, it is useful to reduce it to a sum of Euler characteristics of simpler spaces. This is achieved with the MPS degeneration formula [40] (see also [41]).

Physically speaking, the MPS degeneration formula expresses the bound states as a sum of contributions where the M particles of type one group into clumps, each of which subsequently interact and form bound states with the remaining particles of type two. Weighting each contribution appropriately, we determine that the Euler characteristic of the Kronecker moduli space may be written as

$$\Omega(M, N, k) = \chi(\mathcal{M}^k_{M,N}) = \sum_{m_* \vdash M} \Big[\prod_{\ell=1}^{M} \frac{1}{m_\ell!} \Big(\frac{(-1)^{\ell-1}}{\ell^2} \Big)^{m_\ell} \Big] \chi(\mathcal{M}^k_{m_*,N}), \quad (2.15)$$

where the sum is over all partitions $m_* = (m_1, \ldots, m_M)$ of M,

$$\sum_{\ell=1}^{M} \ell m_\ell = M, \quad m_\ell \in \mathbb{N} \cup \{0\}. \quad (2.16)$$

The main actor in the degeneration formula, is the Euler characteristic of the space $\mathcal{M}^k_{m_*,N}$. This is the quiver moduli space of the "star quiver" (Figure 3) associated to the partition m_*. It has a central non-abelian node with rank N and $\sum_{\ell=1}^{M} m_\ell$ abelian nodes surrounding the non-abelian node. Among all the abelian nodes, m_ℓ of them have ℓk arrows pointing to the non-abelian node for each $\ell = 1, \ldots, M$ (m_ℓ may vanish).
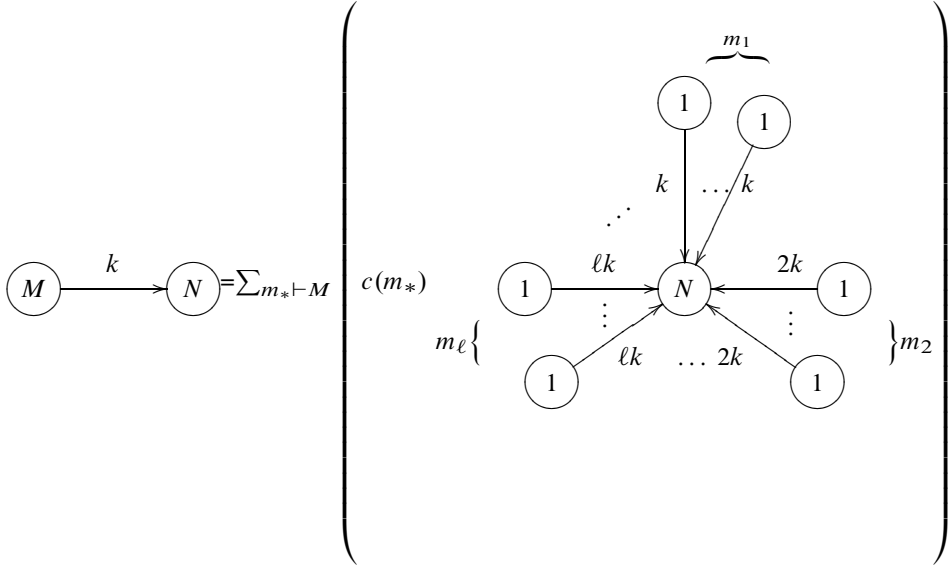
Figure 3. A graphical representation of the MPS degeneration formula (2.15). The Euler characteristic of the Kronecker moduli space can be expressed as a sum of Euler characteristics of star quivers, each associated to a partition of M. The contribution of each star quiver is weighted with a combinatorial coefficient $c(m_*) = \prod_{\ell=1}^{M} \frac{1}{m_\ell!} \left(\frac{(-1)^{\ell-1}}{\ell^2} \right)^{m_\ell}$.

As a result of the degeneration formula (2.15), the task of computing the Euler characteristic of Kronecker moduli space is reduced to determining the Euler characteristics of star quivers. We carry out this task using the supersymmetric localization formula which expresses the Euler characteristic of quiver moduli spaces as a Jeffrey–Kirwan residue integral [11, 12].

In the case of the star quiver associated to the partition $m_* \vdash M$ with general (M, N), the combinatorics of the residues is involved. However in the special case

$$N = Mr + 1, \tag{2.17}$$

for some non-negative integer r, the combinatorics simplifies to an elementary problem in graph theory. From now on, we restrict our analysis to the special case where (2.17) holds. In the remainder of this section we describe the resulting correspondence between residues and graphs, and state the solution to the resulting counting problem. Complete proofs are deferred to §4 and §5 respectively.

In §4, we demonstrate that when $N = Mr + 1$, the Euler characteristic of the star quiver may be expressed as

$$\chi(\mathcal{M}^k_{m_*,Mr+1}) = \frac{1}{(Mr+1)!} T(\vec{L}_{m_*,r}) \prod_{\ell=1}^{M} \left[\binom{\ell k}{\ell r + 1} (\ell r + 1)! \right]^{m_\ell}. \quad (2.18)$$

One significant feature of the above formula is that the k dependence has been solved. Meanwhile, the quantity $T(\vec{L}_{m_*,r})$, is a positive integer depending only on the partition m_*, and the integer r. As we describe in the next subsection, $T(\vec{L}_{m_*,r})$ has a graph theoretic interpretation which enables us to determine it explicitly as well.

2.3. The graph theory problem: counting trees.
In this section, we describe the general graph theory problem to which the quantity $T(\vec{L}_{m_*,r})$ is the solution. The nature of this problem is a direct result of the combinatorics of Jeffrey–Kirwan residues described in §4. A complete treatment of the relevant graph theory (along with proofs omitted here) is given in §5.
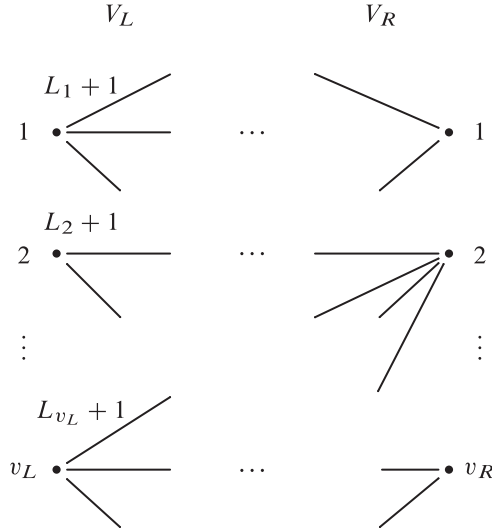
Figure 4. A bipartite graph G in the set $\mathcal{G}(\vec{L})$ defined by a v_L-dimensional vector $\vec{L} = (L_1, \ldots, L_{v_L})$ with $L_i \in \mathbb{N} \cup \{0\}$. (The connections between partite sets are not shown.) There are v_L vertices in V_L and $v_R = 1 + \sum_i L_i$ vertices in V_R. The i-th vertex in V_L is incident to $L_i + 1$ edges. The number of edges for a vertex in V_R is not constrained. The total number of edges is $e = v_L + \sum_i L_i = v_L + v_R - 1$. The quantity of interest $T(\vec{L})$ is the number of trees (connected graphs with no cycle) in the set of bipartite graphs $\mathcal{G}(\vec{L})$.

The graph theory problem of interest concerns counting trees in *bipartite graphs*. Such a graph G is defined by a pair $G = (V_L + V_R, E)$ with V_L and V_R (the *partite sets*) two disjoint sets of vertices and E the set of edges. The bipartite structure means that edges connect vertices in V_L and V_R, but do not connect vertices in the same partite set. The graphs we consider are undirected, meaning that the edges do not have any orientation.

Now, given a positive integer v_L, and $\vec{L} = (L_1, L_2, \ldots, L_{v_L})$ a v_L-dimensional vector with non-negative integral components, we consider bipartite graphs $G = (V_L + V_R, E)$ satisfying the following incidence relations:

- there are v_L vertices in V_L;
- there are $v_R = 1 + \sum_{i=1}^{v_L} L_i$ vertices in V_R;
- there are $L_i + 1$ edges incident to the i-th vertex in V_L.

This definition is asymmetric between the partite sets V_L and V_R. In particular, the graphs in question have an unconstrained number of edges incident at vertices in V_R. We denote the set of bipartite graphs satisfying these incidence data by $\mathcal{G}(\vec{L})$.

Define a *tree,* to be a connected graph with no cycles. The main quantity of interest is then

$$T(\vec{L}) = \text{ number of trees in } \mathcal{G}(\vec{L}). \tag{2.19}$$

The incidence data defining the bipartite graphs $\mathcal{G}(\vec{L})$ are tuned in such a way as to make the number of trees non-zero. Indeed, using $v_R = 1 + \sum_i L_i$, the total number of edges e is related to the total number of vertices $v = v_L + v_R$ by

$$e = \sum_{i=1}^{v_L} (1 + L_i) = v_L + v_R - 1 = v - 1. \tag{2.20}$$

By an elementary proposition in graph theory (see Proposition 1 in §5), a tree has precisely $v - 1$ edges. Hence it is precisely for this choice of v_R that the set of trees can be non-empty. We illustrate these definitions in several examples below.

Example 1 ($v_L = 1$, $\vec{L} = (L_1)$). The simplest example has a single left vertex ($v_L = 1$) and $\vec{L} = (L_1)$ a one-dimensional vector for some non-negative integer L_1. In this case $v_R = L_1 + 1$ and the number of edges $e = L_1 + 1$. For $G \in \mathcal{G}(\vec{L})$, there are $L_1 + 1$ edges incident to the vertex in V_L. There is a unique tree in $\mathcal{G}(\vec{L})$ shown in Figure 5.
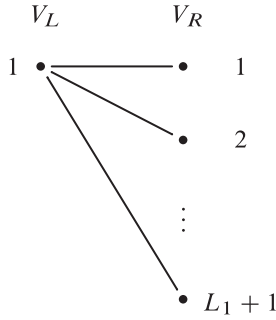
Figure 5. An example of a tree in $\mathcal{G}(\vec{L})$ with $\vec{L} = (L_1)$. We have one vertex in V_L ($v_L = 1$) and $L_1 + 1$ vertices in V_R ($v_R = L_1 + 1$), with a total number of $e = L_1 + 1$ edges. The vertex in V_L is incident to $L_1 + 1$ edges. This is the unique tree in $\mathcal{G}(\vec{L})$, *i.e.* $T(\vec{L}) = 1$.

Example 2 ($v_L = 2$, $\vec{L} = (1,1)$). As a more advanced example, consider the case with two left vertices ($v_L = 2$) and $\vec{L} = (1,1)$ in Figure 6a. There are three right vertices ($v_R = 3$) and four total edges ($e = 4$). Each of the vertices in V_L is incident to 2 edges. There are 6 trees in $\mathcal{G}(\vec{L})$ shown in Figure 6a, *i.e.* $T(\vec{L}) = 6$.
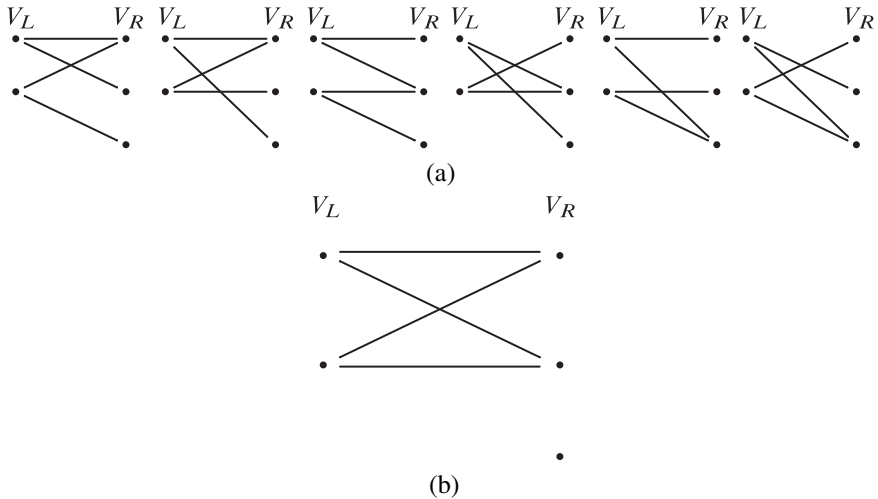
Figure 6. (a) The 6 trees in $\mathcal{G}(\vec{L})$ with $\vec{L} = (1,1)$. (b) A graph in $\mathcal{G}(\vec{L})$ that is not a tree.

2.3.1. The tree counting theorem and $T(\vec{L}_{m_*,r})$. One of the remarkable facts about trees is that given any incidence data defining the set of bipartite graphs $\mathcal{G}(\vec{L})$, the number of trees $T(\vec{L})$ can be exactly determined. The result is a key theorem:

Theorem 1. *The number of trees in the set $\mathcal{G}(\vec{L})$ is*

$$T(\vec{L}) = \frac{(v_R - 1)!}{\prod_{i=1}^{v_L} L_i!} v_R^{v_L - 1}, \tag{2.21}$$

where $v_R = 1 + \sum_{i=1}^{v_L} L_i$.

A proof of this theorem may be found in [42], p. 82.[6] For completeness, in §5 we develop the necessary graph theory to prove (2.21) directly. For now, we apply this result to the problem of the Euler characteristics of star quivers. To do so, it remains to identify the quantity $T(\vec{L}_{m_*,r})$ of (2.18). This is a special case of the tree function $T(\vec{L})$ defined in (2.19).

Given a partition $m_* = (m_1, \ldots, m_M)$ of M, i.e. $m_\ell \geq 0$ and $\sum_\ell \ell m_\ell = M$, and a non-negative integer r, we associate the following choice of the vector $\vec{L}$:

$$\vec{L}_{m_*,r} = \Big(\underbrace{r, \ldots, r}_{m_1}, \ldots, \underbrace{\ell r, \ldots, \ell r}_{m_\ell}, \ldots, \underbrace{Mr, \ldots, Mr}_{m_M} \Big). \tag{2.22}$$

The number of vertices and edges in such trees are read off from the above. We have

$$v_L = \sum_{\ell=1}^{M} m_\ell, \quad v_R = Mr + 1, \quad e = Mr + \sum_{\ell=1}^{M} m_\ell. \tag{2.23}$$

These quantities are related to the physical parameters defining the star quiver of Figure 3. In particular, v_L is the number of abelian nodes, while v_R is the rank of the central non-abelian node. Finally, the structure of $\vec{L}_{m_*,r}$ emerges from the pattern of Fayet–Iliopoulos parameters as derived in §4.

Applying the tree counting Theorem 1 we conclude that the number of bipartite trees with this incidence data is given by

$$T(\vec{L}_{m_*,r}) = \frac{(Mr)!}{\prod_{\ell=1}^{M} (\ell r)!^{m_\ell}} (Mr + 1)^{\sum_\ell m_\ell - 1}. \tag{2.24}$$

---

[6] We thank Fan Wei and Yu-Wei Fan for bringing this reference to our attention.

2.4. An index formula for the Kronecker quiver $(M, Mr + 1)$. Armed with an explicit expression for $T(\vec{L}_{m_*,r})$ and the factorization formula (2.18), we are now ready to present our main result. The index for the Kronecker quiver quantum mechanics with dimension vector $(M, Mr + 1)$ and k arrows is

$$
\chi(\mathcal{M}^k_{M,Mr+1})
$$
$$
= \frac{1}{(Mr+1)^2} \sum_{m_* \vdash M} \prod_{\ell=1}^{M} \frac{1}{m_\ell!} \left[\frac{(-1)^{\ell-1}}{\ell^2} \binom{\ell k}{\ell r + 1} (Mr+1)(\ell r + 1) \right]^{m_\ell},
$$
(2.25)

where the sum is over the partitions $m_* = (m_1, m_2, \ldots, m_M)$ of M, *i.e.* $\sum_\ell \ell m_\ell = M$ and $m_\ell \in \mathbb{N} \cup \{0\}$.

The expression (2.25) may be simplified with the help of an exponential resummation and the introduction of a generating function. Introduce the function

$$
F(k, r, x) = (k - r) \sum_{\ell=1}^{\infty} \frac{(-1)^{\ell-1}}{\ell} \binom{k\ell}{r\ell} x^\ell,
$$
(2.26)

and let $[x^j]\{q(x)\}$ denote the coefficient of x^j in a power series $q(x)$. Then, using the identity

$$
\sum_{M=0}^{\infty} \sum_{m_* \vdash M} \prod_{\ell=1}^{M} \frac{1}{m_\ell!} (p(\ell) x^\ell)^{m_\ell} = \exp\left[\sum_{\ell=1}^{\infty} p(\ell) x^\ell \right],
$$
(2.27)

we can express (2.25) as

$$
\boxed{
\begin{aligned}
\Omega(M, Mr + 1, k) &= \chi(\mathcal{M}^k_{M,Mr+1}) \\
&= \frac{1}{(Mr+1)^2} [x^M]\{\exp[(Mr+1)F(k, r, x)]\}.
\end{aligned}
}
$$
(2.28)

This is our final result for the general Euler characteristic of Kronecker moduli space.

3. Analysis of the index formula

In this section, we provide a number of checks on the index formula.

In §3.1 we illustrate simplifications that occur in the index formula at special values of r. Specifically, we recover the Grassmannian index at $r = 0$ and determine a closed form expression for the degeneracies when $r = 1$. In §3.2 we

demonstrate that the index formula satisfies required symmetry properties arising from isomorphisms of Kronecker moduli spaces. Finally, in §3.3, we directly compare our index result (2.28) to wall-crossing formulas.

3.1. Simplifications at special values of r. In this section we describe simplifications to the Euler characteristic formula which occur at special values of r.

3.1.1. Recovering the Grassmannian index. The first check on our result occurs when $r = 0$. In that case the dimension vector is $(M, 1)$ and hence as reviewed in §2.1.1, the moduli space is a Grassmannian. Thus, for $r = 0$ we must recover $\chi(\mathrm{Gr}(M, k))$. This is readily verified. Indeed, when $r = 0$, the function $F(k, r = 0, x)$ of (2.26) simplifies to

$$F(k, r = 0, x) = k \sum_{\ell=1}^{\infty} \frac{(-1)^{\ell-1}}{\ell} x^\ell = k \log(1 + x). \tag{3.1}$$

The Euler characteristic of the quiver moduli space $\mathcal{M}_{M,1}^k$ is then determined from the prescription (2.28) as

$$\chi(\mathcal{M}_{M,1}^k) = [x^M]\{\exp[F(k, 0, x)]\} = [x^M]\{(1 + x)^k\} = \binom{k}{M}, \tag{3.2}$$

which is indeed the Euler characteristic for the Grassmannian $\mathrm{Gr}(M, k)$.

3.1.2. The case $r = 1$. The index formula (2.28) also simplifies in the special case $r = 1$ (as well as the equivalent case $r = k - 1$ via (3.11)).

In that case, the function $F(k, 1, x)$ of (2.26) may be rewritten in terms of the *generalized binomial series* $\mathcal{B}_k(x)$ defined as [43]

$$\mathcal{B}_k(x) = \sum_{\ell=0}^{\infty} \binom{k\ell + 1}{\ell} \frac{x^\ell}{k\ell + 1}. \tag{3.3}$$

The generalized binomial series obeys an algebraic identity

$$\mathcal{B}_k(x) = 1 + x\mathcal{B}_k(x)^k, \tag{3.4}$$

which enables one to easily determine the power series coefficients of $\mathcal{B}_k(x)$ raised to an arbitrary real power

$$[x^m]\{\mathcal{B}_k(x)^s\} = \binom{mk + s}{m} \frac{s}{mk + s}. \tag{3.5}$$

In particular, in the $s \to 0$ limit we then obtain

$$\log(\mathcal{B}_k(x)) = \sum_{\ell=1}^{\infty} \binom{k\ell}{\ell} \frac{x^\ell}{k\ell}. \tag{3.6}$$

From which we deduce that

$$\exp[F(k, 1, x)] = \mathcal{B}_k(-x)^{k(1-k)}. \tag{3.7}$$

Comparison to the index formula (2.28), now yields the following simple expression for the index

$$\Omega(M, M+1, k) = \chi(\mathcal{M}_{M,M+1}^k)$$
$$= \frac{k}{(M+1)[(k-1)M + k]} \binom{(k-1)^2 M + k(k-1)}{M}. \tag{3.8}$$

The result (3.8) was first obtained by Weist [8] by alternative techniques. The fact that we have reproduced (3.8) using the combinatorics of Jeffrey–Kirwan residues provides a strong check on our method.

Beyond the direct check provided on our work, the appearance of the generalized binomial series is in and of itself significant. This function, $\mathcal{B}_k(x)$, has a natural combinatorial interpretation as the generating function of rooted k-ary trees. These binomials series also make an appearance in the generating function of indices $\Omega(M, M, k)$, see [3, 4, 6]. In that case, since the dimension vector (M, M) is not coprime, the quiver quantum mechanics has bound states at threshold. The associated Kronecker quiver moduli spaces have singularities, and extracting the indices from geometry is delicate. Nevertheless, the resulting generating function again involves the generalized binomial series and suggests a direct interpretation of the index and bound states in terms of rooted trees, perhaps as attractor flow trees [33, 34].

3.2. Symmetries of the index formula. As a further consistency check, in this section we show our formula (2.28) respects the isomorphisms of the quiver moduli space (2.6):

$$\Omega(M, N, k) = \Omega(N, M, k),$$
$$\Omega(M, N, k) = \Omega(N, Nk - M, k). \tag{3.9}$$

Among all the isomorphisms, the following two infinite families are of particular interest.

$$\Omega(2, 2r+1, k) = \Omega(2, 2(k-r-1)+1, k), \tag{3.10}$$

and

$$\Omega(M, M + 1, k) = \Omega\left(M + 1, (k - 1)(M + 1) + 1, k\right). \qquad (3.11)$$

This is because the dimension vectors on both sides of the isomorphisms are of the special case $N = Mr + 1$, for which our formula (2.28) is applicable. We will explicitly prove the invariance of our formula (2.28) in the following.

The first isomorphism. For the first isomorphism (3.10), it is easier to use the alternative expression (2.25) for our formula for the index. Using (2.25), the left-hand-side of (3.10) becomes

$$\Omega(2, 2r + 1, k) = -\frac{1}{4}\binom{2k}{2r + 1} + \frac{1}{2}\left[\frac{k!}{r!(k - r - 1)!}\right]^2. \qquad (3.12)$$

Similarly, the righthand side of (3.10) may be written as

$$\Omega(2, 2(k - r - 1) + 1, k) = -\frac{1}{4}\binom{2k}{2k - 2r - 1} + \frac{1}{2}\left[\frac{k!}{(k - r - 1)!r!}\right]^2, \quad (3.13)$$

which is manifestly the same as (3.12).

The second isomorphism. The second isomorphism (3.11) is harder to prove. First let us note the following identity from the definition of $F(k, r, x)$ (2.26),

$$F(k, k - 1, x) = \frac{1}{k - 1}F(k, 1, x). \qquad (3.14)$$

Applying our general formula (2.28) to the righthand side of (3.11) , we have

$$\Omega(M + 1, (k - 1)(M + 1) + 1, k)$$
$$= \frac{1}{[(k - 1)(M + 1) + 1]^2}[x^{M+1}]\left\{\exp\left[\left(M + 1 + \frac{1}{k - 1}\right)F(k, 1, x)\right]\right\}, \qquad (3.15)$$

where we have used the identity (3.14).

The relationship between F and the generalized binomial series in the case $r = 1$ stated in equation (3.7) (as well as the direct argument given in Appendix A) shows that function $F(k, r, x)$ satisfies the following identity

$$[x^M]\{\exp[\beta F(k, 1, x)]\} = \frac{\beta}{M}k(k - 1)\binom{k(k - 1)\beta - (k - 1)M - 1}{M - 1}, \quad (3.16)$$

for any complex number β. Applying (3.16) with $\beta = M + 1 + \frac{1}{k-1}$ to (3.15), we have

$$\begin{aligned}
&\Omega(M + 1, (k-1)(M+1) + 1, k) \\
&\quad = \frac{1}{(k-1)M + k}\left((k-1)^2 M + k(k-1)\right)^{\frac{k}{M+1}} M \\
&\quad = \Omega(M, M+1, k),
\end{aligned}$$ (3.17)

where in the last equality we have used the simplified expression (3.8) in the case $r = 1$. Hence we have checked that our formula (2.28) respects the isomorphisms (2.6).

3.3. Comparison to wall-crossing formulas.

A final check on our results is to directly compare the output to wall-crossing formulas. This allows us to check our result (2.28) for general r and for M and k sufficiently small.

The wall-crossing formula of [3] allows us to determine the change in the indices $\Omega(M, N, k)$ as the Fayet–Iliopoulos parameters ζ are varied. Mathematically, this is the change in the Donaldson–Thomas invariants of the quiver, as the stability condition is changed.

In the context of the Kronecker model, the wall-crossing formula is particularly simple to apply. By changing the sign of the FI parameter ζ of (2.2), we reach a chamber where all moduli spaces are empty, and no non-trivial bound states can form. The only stable states are then a single particle of type one, or a single particle of type two. We may use this simple chamber ($\zeta < 0$) as a seed and apply the wall-crossing formula to determine the indices in the chamber of interest ($\zeta > 0$).

To phrase the wall-crossing computation we first introduce functions $K_{M,N}$ which act on formal variables $[x, y]$ as

$$K_{M,N}[x, y] = [x(1 - (-1)^{kMN} x^M y^N)^{kN}, y(1 - (-1)^{kMN} x^M y^N)^{-kM}]. \quad (3.18)$$

We also introduce a sign function which detects the parity of the dimension of $\mathcal{M}_{M,N}^k$

$$\sigma(M, N, k) = \begin{cases} +1, & kMN - M^2 - N^2 + 1 \equiv 0 \ (\mathrm{mod}\ 2), \\ -1, & kMN - M^2 - N^2 + 1 \equiv 1 \ (\mathrm{mod}\ 2). \end{cases} \quad (3.19)$$

The wall-crossing formula asserts that a particular function of $[x, y]$ built via compositions of the above functions does not depend on the chamber. In the case

at hand this implies that

$$\overrightarrow{\prod_{M,N \geq 0}} K_{M,N}^{\sigma(M,N,k)\Omega(M,N,k)} = K_{0,1} \circ K_{1,0}, \qquad (3.20)$$

Where in the above, the product operation is composition of functions, and the order of composition is that of decreasing[7] M/N.

   To use the wall-crossing formula, note that the function $K_{M,N}$ differs from the identity only at order $x^M y^N$. Whence if we fix a positive integer Q we may solve (3.20) order by order by replacing the infinite product with a finite product where only those $K_{M,N}$ are retained with $M + N \leq Q$. Then we may compute the composition as a formal power series (again only retaining terms differing from the identity up to total order Q). Matching to the right-hand side, we then solve for all $\Omega(M, N, k)$ with $M + N \leq Q$.

   This procedure is computationally costly to carry out for large Q. However, for Q sufficiently small, wall-crossing provides a useful crosscheck on our results in the case where $r \neq 0, 1$. As an example in Table 1, we present wall-crossing results for $r = 2$. All indices computed thus far agree with our general index prescription (2.28), and provides a strong check on the validity of our result.

Table 1. Indices $\Omega(M, Mr + 1, k)$, extracted from the wall-crossing formula for $r = 2$ and various values of k and M. The data agrees with our general index formula.

r=2	$k = 4$	$k = 5$	$k = 6$
$M = 0$	1	1	1
$M = 1$	4	10	20
$M = 2$	58	387	1602
$M = 3$	1264	22765	196136
$M = 4$	33751	1647265	29595451
$M = 5$	1018252	134924271	5059514952
$M = 6$	33331794	12003007130	939887566862
$M = 7$	1156714720	1132713788250	185267731189312
$M = 8$	41942224979	111732981265605	38180107620131049
$M = 9$	1573700333920	11407942652134355	8145089457477277400
$M = 10$	60685423064290	1197321303724493265	1786374698749585024792
$M = 11$	2393245242889696	128534027591027982405	400759043478342386735448
$M = 12$	96164522270610418	14060437197335739888902	91619999838823992655697998
$M = 13$	3925754745132237556	1562780288066103516885980	21283030090887836618088693536

---

[7] If $M_1/N_1 = M_1/N_2$ then $K_{M_1,N_1} \circ K_{M_2,N_2} = K_{M_2,N_2} \circ K_{M_1,N_1}$. Also the need to introduce σ is because we have defined the index Ω to coincide with the Euler characteristic.

4. Bipartite graphs from contour integrals

In this section we derive the graph theory algorithm to compute the refined index of star quivers illustrated in Figure 7 using a Jeffrey–Kirwan residue formula.

We start in §4.1 with a presentation of the residue formula for the index of star quivers as derived by supersymmetric localization. In §4.2 we begin our task of enumerating the poles that contribute to the residue formula. In §4.3 we demonstrate that every contributing pole corresponds to a choice of a bipartite graph. Finally, in §4.4 we prove that each graph associated to a pole in the index is a tree described by the incidence data used in §2.3. In particular we derive the Euler characteristic of the star quiver (4.19).
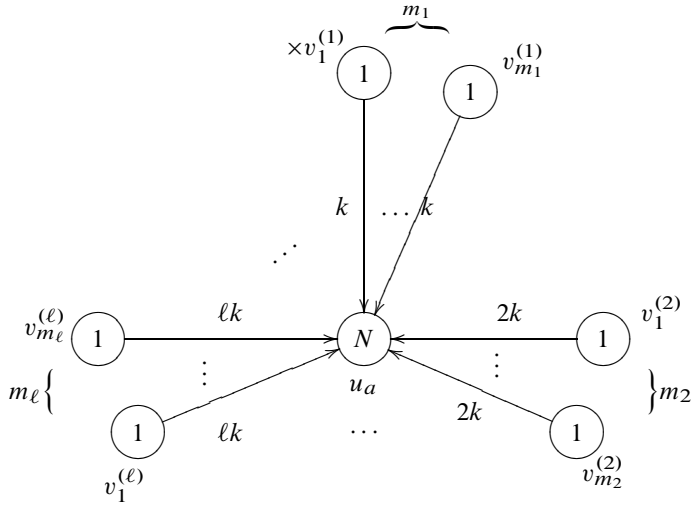
Figure 7. The "star quiver" associated to the partition $m_* = (m_1, \ldots, m_M)$ of M. There is a single non-abelian node with rank N and $\sum_{\ell=1}^{M} m_\ell$ abelian nodes surrounding the non-abelian node. Among all the abelian nodes, m_ℓ of them have ℓk arrows pointing to the non-abelian node for each $\ell = 1, \ldots, M$ (m_ℓ could be zero). The gauge fugacities of the non-abelian node are denoted by u_a, $a = 1, \ldots, N$, while those of the abelian nodes are denoted by $v_I^{(\ell)}$ with $\ell = 1, \ldots, M$ and $I = 1, \ldots, m_\ell$. The cross $\times$ for $v_1^{(1)}$ means that abelian node is decoupled when we apply the residue formula.

4.1. A residue for the star quiver.
In this section, we introduce the residue formula for the refined index of the star quiver.

We begin with a recollection of the data of the star quiver and introduce the relevant notation.

Let e denote the total rank of the gauge group of the star quiver.[8] The residue formula that we use to compute cohomology of star quivers has e integration variables (known as gauge fugacities). We label them as follows.

- The gauge fugacities of the central non-abelian node of the star quiver are indicated by u_a, $a = 1, \ldots, N$.

- There are m_ℓ abelian nodes in the star quiver which each has ℓk arrows to the central non-abelian node. Thus we may label the abelian nodes by a pair of integers (I, ℓ) with $\ell = 1, \ldots, M$ and $I = 1, \ldots, m_\ell$. Correspondingly, we indicate the gauge fugacity of an abelian node by $v_I^{(\ell)}$.

Next, consider the node (I, ℓ). This node has ℓk identical arrows emanating from it. As a result, the quantum mechanics has an $SU(\ell k)$ flavor symmetry acting on these chiral multiplets in fundamental representation. Mathematically, this means that the moduli space is acted on by $SU(\ell k)$. We may introduce fixed flavor fugacities into the contour integral (i.e. we may work equivariantly with respect to this action).

- The flavor fugacities associated to the $SU(\ell k)$ flavor symmetry acting on nodes emanating from the node (I, ℓ), are denoted by $\xi_i^{(I, \ell)}$ with $i = 1, \ldots, \ell k$. We choose these flavor fugacities to be generic complex numbers. In particular, this means that the $\xi_i^{(I, \ell)}$ are linearly independent over the rational numbers. Thus, any relation of the form

$$\sum q_i^{(I, \ell)} \xi_i^{(I, \ell)} = 0, \tag{4.1}$$

with rational $q_i^{(I, \ell)}$ implies that all $q_i^{(I, \ell)}$ vanish.

It is important that the refined index $\Omega(\mathcal{M}_{m_*, N}^k, y)$ in fact does not depend on the flavor fugacities due to the $\mathcal{N} = 4$ supersymmetry [12]. Our purpose in introducing these variables is to separate multiple poles in contour integrals and turn the residue calculation into a combinatorics problem.

Finally, before introducing the residue integral, we recall an important technical point. To compute the refined index of the quiver quantum mechanics, we must decouple a $u(1)$ vector multiplet; otherwise the fermionic zero modes of the overall $u(1)$ would make the answer zero.[9] The index does not depend on which $u(1)$ we decouple. For concreteness, we will decouple the $(I = 1, \ell = 1)$-th

---

[8] As we shall demonstrate, e is also the number of edges in the bipartite trees relevant to the residue, hence the choice of notation.

[9] This is due to the fact that all mater transforms in adjoints and bifundamentals, thus an overall $u(1)$ in the gauge group, decouples.

abelian node whose gauge fugacity is[10] $v_1^{(1)}$. In the following, $v_1^{(1)}$ is interpreted to vanish when it appears in equations.

We are now prepared to introduce the residue formula for the index. According to the general supersymmetric localization arguments of [10–12] the index may be expressed as[11]

$$
\begin{aligned}
&\Omega(\mathcal{M}_{m_*,N}^k, y) \\
&= \left(\frac{1}{\sin(z)}\right)^e \sum_{(u_*,v_*)\in\mathfrak{M}_{\text{sing}}^*} \underset{(u,v)=(u_*,v_*)}{\text{JK-Res}} (\mathbf{Q}(u_*,v_*),\zeta) Z_{\text{1-loop}}(u,v,z,\xi),
\end{aligned}
\tag{4.2}
$$

where $y = e^{iz}$, and e is the rank of the star quiver after decoupling an overall $U(1)$:

$$
e = N + \sum_{\ell=1}^{M} m_\ell - 1.
\tag{4.3}
$$

The above result (4.2) arises from localization of a path integral defining the quantum mechanics partition function. It is an intrinsically Coulomb branch formula, i.e. it expresses the desired Hirzebruch χ_y genera in terms of contour integrals over auxiliary parameters (vector multiplet fields) that are not visible to Higgs branch physics where the geometry of the moduli space is manifest. The advantage of this technique is that the entire complexity of the quiver representation moduli space is bypassed, and only relevant information for computing the χ_y genus is retained and packaged into the integrand discussed in detail below. We refer to section 4 of [12] for a first principles derivation of this result (building on earlier work in [44,45]), and to [11] for elementary examples of applications to quiver representation theory.

Let us describe in detail the elements of the residue formula (4.2).

- The one-loop determinant $Z_{\text{1-loop}}$ is[12]

$$
\begin{aligned}
&Z_{\text{1-loop}}(u,v,z,\xi) \\
&= \frac{1}{N!} \prod_{\substack{a,b=1 \\ a\neq b}}^{N} \frac{\sin(u_a - u_b)}{\sin(u_a - u_b + z)} \prod_{a=1}^{N} \prod_{\ell=1}^{M} \prod_{I=1}^{m_\ell} \prod_{i=1}^{\ell k} \frac{\sin(u_a - v_I^{(\ell)} - \xi_i^{(I,\ell)} + z)}{\sin(u_a - v_I^{(\ell)} - \xi_i^{(I,\ell)})},
\end{aligned}
\tag{4.4}
$$

---

[10] For partitions with vanishing m_1, one must decouple an alternate choice of gauge fugacity $v_I^{(\ell)}$. As we will ultimately see, the symmetry between the nodes, including the decoupled one, is restored. Thus, the choice of which node one decouples is irrelevant.

[11] We have suppressed the dependence of Ω on the FI parameter ζ since we are only interested in the choice (4.5).

[12] We use a slightly different conventions on u and z than in [11]. $u_{\text{here}} = \pi u_{\text{there}}$ and $z_{\text{here}} = -\pi z_{\text{there}}$.

- The FI parameter $\zeta \in \mathbb{C}^e$ is determined by the MPS formula [40] to be

$$
\zeta = \Big(\underbrace{1, \ldots, 1}_{N}, \underbrace{-\frac{1}{M}N, \ldots, -\frac{1}{M}N}_{m_1 - 1}, \underbrace{-\frac{2}{M}N, \ldots, -\frac{2}{M}N}_{m_2}, \ldots,
$$
$$
\underbrace{-\frac{\ell}{M}N, \ldots, -\frac{\ell}{M}N}_{m_\ell}, \ldots \Big),
$$

(4.5)

where we order the variables as $(u_a, v_I^{(1)}, v_I^{(2)}, \ldots, v_I^{(\ell)}, \ldots, v_I^{(M)})$. Again, we only have $m_1 - 1$ components equal to $-1/M$ because one of the abelian node with k arrows is decoupled. Notice that if we had not decoupled the $u(1)$, the sum of the components of ζ would be $N \times \frac{1}{N} - \sum_\ell m_\ell \times \frac{\ell}{M} = 0$, indicating that the overall $u(1)$ decouples.

- The summation is over points (u_*, v_*) in the gauge fugacity space where at least e of the sine factors appearing in the denominator of (4.4) vanish. These are poles which may contribute to the residue extracted by the operator JK-Res. We explain this operator in detail in the following subsection.

4.2. The Jeffrey–Kirwan rule. In this section, we describe the residue operator JK-Res which specifies the contribution of a given pole point (u_*, v_*) in the gauge fugacity space. We refer to the resulting rule dictating which poles contribute to the index as the "Jeffrey–Kirwan rule."

Consider a given polar point (u_*, v_*). This pole is said to be *non-degenerate* if there are exactly e denominator factors in (4.4) which vanish at (u_*, v_*). Meanwhile, if more than e denominator factors in (4.4) vanish at (u_*, v_*) the pole is said to be *degenerate*.

For general M, N, both the degenerate and non-degenerate poles contribute to the index. However, in the case

$$
N = Mr + 1, \tag{4.6}
$$

for some non-negative integer r, we conjecture that only the non-degenerate poles contribute. We argue for this significant technical simplification in Appendix B. The fact that our final results agree with indices produced from wall-crossing in Section 3.3 gives strong evidence for the consistency of this assumption. In the remainder of our analysis, we restrict to the case where (4.6) holds. Our task is thus reduced to describing the non-degenerate poles.

At each non-degenerate pole (u_*, v_*), there are exactly e denominator factors that vanish at (u_*, v_*). Each such denominator factor is a sine function whose argument is a linear function of the gauge and flavor fugacities. The dependence on the gauge fugacities is conveniently encoded by a vector Q composed of the coefficients of the gauge fugacities in the arguments of the sine function. A non-degenerate pole is thus associated to e such vectors $Q_1, \ldots, Q_e$. We denote the collection of these e vectors as $\mathbf{Q}(u_*, v_*)$.

For each non-degenerate pole, the Jeffrey–Kirwan residue operator may be conveniently phrased in terms of the associated vectors $\mathbf{Q}(u_*, v_*)$. First, define the positive cone of the vectors $\mathbf{Q}(u_*, v_*)$, to be those vectors that may be expressed as linear combinations of the Q_i with positive real coefficients. We denote this cone as $\mathrm{Cone}(\mathbf{Q}(u_*, v_*))$. Then, the Jeffrey–Kirwan residue operator is

$$
\begin{aligned}
\underset{(u,v)=(u_*,v_*)}{\mathrm{JK\text{-}Res}} & (\mathbf{Q}(u_*, v_*), \zeta) \, \frac{1}{Q_1(u, v)} \cdots \frac{1}{Q_e(u, v)} \\
&= \begin{cases} \det |(Q_1 \ldots Q_e)|^{-1}, & \zeta \in \mathrm{Cone}(\mathbf{Q}(u_*, v_*)), \\ 0, & \zeta \notin \mathrm{Cone}(\mathbf{Q}(u_*, v_*)). \end{cases}
\end{aligned}
\tag{4.7}
$$

Thus, to evaluate the general residue formula (4.2) we must enumerate the non-degenerate poles with $\zeta \in \mathrm{Cone}(\mathbf{Q}(u_*, v_*))$. To determine the full y-dependent index of the star quiver (4.2), we then sum the resulting contributions from each pole. We carry this out explicitly in §6. Meanwhile, in the special case of the Euler characteristic ($y = 1$) it is easy to see that each pole with $\zeta \in \mathrm{Cone}(\mathbf{Q}(u_*, v_*))$ contributes exactly $1/(Mr + 1)!$ to $\chi(\mathcal{M}^k_{m_*, Mr+1})$. Evaluating the Euler characteristic is therefore reduced to the combinatorial enumeration of contributing poles.

We begin our task of tallying these poles by examining the FI parameter. In the case $N = Mr + 1$ of interest this takes the form

$$
\begin{aligned}
\zeta = \Big(\underbrace{1, \ldots, 1}_{N}, & \underbrace{-\Big(r + \frac{1}{M}\Big), \ldots, -\Big(r + \frac{1}{M}\Big)}_{m_1 - 1}, \\
& \underbrace{-\Big(2r + \frac{2}{M}\Big), \ldots, -\Big(2r + \frac{2}{M}\Big)}_{m_2}, \ldots, \\
& \underbrace{-\Big(\ell r + \frac{\ell}{M}\Big), \ldots, -\Big(\ell r + \frac{\ell}{M}\Big)}_{m_\ell}, \ldots \Big).
\end{aligned}
\tag{4.8}
$$

A contributing pole is defined by choosing e factors in the denominator of (4.4), and we aim to constrain admissible choices.

First of all, it is easy to see that we can never have a contributing pole where one of the vanishing sine factors is $\sin(u_a - u_b)$, as in that case the associated vector Q is orthogonal to ζ. Next, note that when we write ζ as a positive linear combination of the Q vectors corresponding to[13] $\sin(u_a - v_I^{(\ell)} - \xi_i^{(I,\ell)})$ and $\sin(u_a - \xi_i^{(1,1)})$, the coefficients are less than or equal to 1; otherwise the components of ζ corresponding to u_a would exceed 1. Examining the coefficient of $v_I^{(\ell)}$, it then follows that we have to pick at least $\ell r + 1$ factors of the form $\sin(u_a - v_I^{(\ell)} - \xi_i^{(I,\ell)})$ for some $a = 1, \ldots, N$ and $i = 1, \ldots, \ell k$.

We now show that $\ell r + 1$ is exactly the number of sines we need to pick to correctly account for the coefficient of $v_I^{(\ell)}$. Suppose we have picked $\ell r + 1 + \delta^{(I,\ell)}$ factors $\sin(u_a - v_I^{(\ell)} - \xi_i^{(I,\ell)})$ for each (I, ℓ) with $\delta^{(I,\ell)} \geq 0$. We argue that $\delta^{(I,\ell)} = 0$. We must select the remaining sine factors to be of the form $\sin(u_a - \xi_i^{(1,1)})$. The remaining number of sine factors to choose is

$$e - \sum_{(I,\ell) \neq (1,1)} (\ell r + 1 + \delta^{(I,\ell)}) = (r + 1) - \sum_{(I,\ell) \neq (1,1)} \delta^{(I,\ell)}. \tag{4.9}$$

Now the sum of the N components corresponding to u_a is

$$(r + 1) - \sum_{(I,\ell) \neq (1,1)} \delta^{(I,\ell)} + \sum_{(I,\ell) \neq (1,1)} \left(\ell r + \frac{\ell}{M} \right) = Mr + 1 - \sum_{(I,\ell) \neq (1,1)} \delta^{(I,\ell)}. \tag{4.10}$$

On the other hand, the sum of the components corresponding to u_a for the FI parameter ζ (see (4.8)) is $N = Mr + 1$. It follows that $\delta^{(I,\ell)} = 0$.

To summarize, for each (I, ℓ), we have to pick precisely $\ell r + 1$ factors of the form $\sin(u_a - v_I^{(\ell)} - \xi_i^{(I,\ell)})$. Meanwhile, we have to pick $r + 1$ factors of the form $\sin(u_a - \xi_i^{(1,1)})$ which we may view as being associated to the decoupled node. This is the same number had the node not been decoupled. We thus see that in the case $N = Mr + 1$, the decoupled node is treated on the same footing as the others. This gives the Jeffrey–Kirwan rule:

JK rule. For a given (I, ℓ), we need to pick exactly $(\ell r + 1)$ factors of the form $\sin(u_a - v_I^{(\ell)} - \xi_i^{(I,\ell)})$ in the denominator of (4.4) for the pole to make a non-zero contribution to the residue.

4.3. From poles to bipartite graphs. We are now ready to enumerate all the poles satisfying the Jeffrey–Kirwan rule. It turns out that the resulting combinatorics problem has a natural interpretation in graph theory. In this section we describe the dictionary between a contributing pole and a bipartite graph.

---

[13] Recall that we have decoupled a node that would have had gauge fugacity $v_1^{(1)}$. The factor $\sin(u_a - \xi_i^{(1,1)})$ in $Z_{\text{1-loop}}$ corresponds to the chiral multiplet connected to this decoupled node.

We begin with the choices of the flavor fugacities $\xi_i^{(I,\ell)}$ appearing in the sine factors. Different choices of flavor fugacities will *not* be reflected as different bipartite graphs which we introduce. Given a group of arrows emanating from the node (I, ℓ), the choices for the flavor fugacities are easy to enumerate and will be considered a trivial factor.

Indeed, the only rule for choosing the flavor fugacities is that if the ξ's in two sine factors are the same, then the residue for that pole is zero. For example, if we pick both

$$\sin(u_1 - v_I^{(\ell)} - \xi_1^{(I,\ell)}), \quad \sin(u_2 - v_I^{(\ell)} - \xi_1^{(I,\ell)}),$$

it follows that $u_1 = u_2$ at this pole. The residue for this pole is then zero due to the factor $\sin^2(u_1 - u_2)$ in the numerator of (4.4). Hence for each group of arrows labels by (I, ℓ), we have to pick $\ell r + 1$ distinct ξ (with order) out of the ℓk of them. This results in the following factor

$$\prod_{\ell=1}^{M}\left[\binom{\ell k}{\ell r + 1}(\ell r + 1)!\right]^{m_\ell}. \tag{4.11}$$

Next, we must choose which u_a's are in the selected $\sin(u_a - v_I^{(\ell)} - \xi)$ factors.[14] We represent these choices by a bipartite graph $G = (V_L + V_R, E)$ with V_L and V_R being the two disjoint sets of vertices and E being the set of edges.

The set of bipartite graphs of interest is $\mathcal{G}(\vec{L}_{m_*, r})$ introduced in §2.3. For a bipartite graph in $\mathcal{G}(\vec{L}_{m_*, r})$, it has $v_L = \sum_\ell m_\ell$ vertices in V_L and $v_R = N = Mr + 1$ vertices in V_R. We will label the vertex in V_L by a pair of integers[15] (I, ℓ) with $I = 1, \ldots, m_\ell$ and $\ell = 1, \ldots, M$. For $G \in \mathcal{G}(\vec{L}_{m_*, r})$, the (I, ℓ)-th vertex in V_L is incident to $\ell r + 1$ edges. The total number of edges e is therefore

$$e = \sum_{\ell=1}^{M} m_\ell(\ell r + 1) = Mr + \sum_{\ell=1}^{M} m_\ell, \tag{4.12}$$

which is again the total rank of the star quiver.

We may now translate every pole for the star quiver associated to the partition m_* into a bipartite graph in $\mathcal{G}(\vec{L}_{m_*, r})$:

- each vertex in V_L corresponds to a gauge fugacity $v_I^{(\ell)}$ of the (I, ℓ)-th abelian node;

---

[14] We will not write the superscript for the flavor fugacities from now on as the number of choices have been enumerated in (4.11).

[15] If $m_\ell = 0$, then we do not have the corresponding vertex.

- each vertex in V_R corresponds to a gauge fugacity u_a of the non-abelian node;
- an edge between the (I, ℓ)-th vertex in V_L and the a-th vertex in V_R corresponds to a pole satisfying $u_a - v_I^{(\ell)} - \xi = 0$.

To specify a non-degenerate pole, we have to pick e sine factors. In the language of bipartite graph, we have to draw precisely e edges. The resulting geometry is indicated in Figure 8.
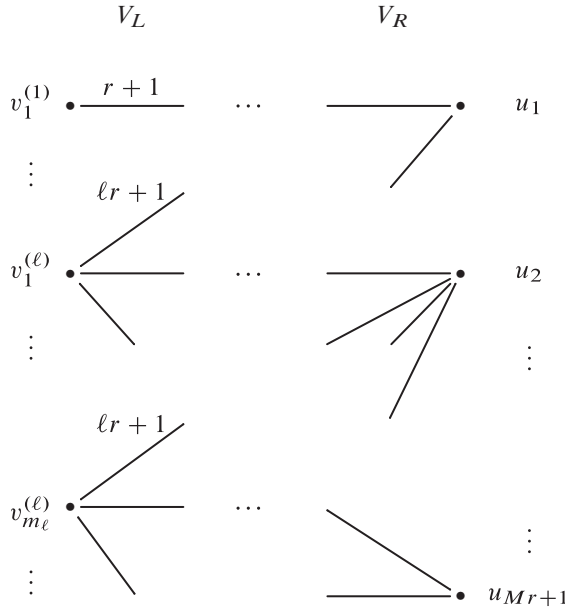
Figure 8. Each pole (modulo the flavor fugacity degeneracy (4.11)) for the star quiver $\mathcal{M}_{m_*, Mr+1}^k$ satisfying the Jeffrey–Kirwan rule corresponds to a bipartite graph G in the set $\mathcal{G}(\vec{L}_{m_*, r})$ with $\vec{L}_{m_*, r}$ given in (2.22). Each vertex in V_L corresponds to a gauge fugacity for the abelian node $v_I^{(\ell)}$, with $I = 1, \ldots, m_\ell$ ($v_I^{(\ell)}$ does not exist if $m_\ell = 0$), while each vertex in V_R corresponds to a gauge fugacity for the non-abelian node u_a, $a = 1, \ldots, Mr + 1$. There are $v_L = \sum_\ell m_\ell$ vertices in V_L and $v_R = Mr + 1$ vertices in V_R. The (I, ℓ)-th vertex in V_L is incident to $\ell r + 1$ edges. The number of edges for a vertex u_a in V_R is not constrained. The total number of edges is $e = Mr + \sum_\ell m_\ell$. The main quantity of interest $T(\vec{L}_{m_*, r})$ is the number of trees (connected graphs with no cycle) in this set of bipartite graphs $\mathcal{G}(\vec{L}_{m_*, r})$.

As an example of the correspondence between poles and graphs, consider for $r = 1$ and $\ell = 3$, a choice of denominator factors

$$\sin(u_1 - v_I^{(3)} - \xi), \quad \sin(u_2 - v_I^{(3)} - \xi),$$
$$\sin(u_5 - v_I^{(3)} - \xi), \quad \sin(u_8 - v_I^{(3)} - \xi). \tag{4.13}$$

This corresponds to the bipartite subgraph in Figure 9. Note that we have $\ell r + 1 = 4$ edges incident to the vertex $v_I^{(3)}$.
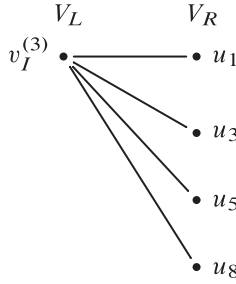
Figure 9. A bipartite subgraph corresponds to the choice of vanishing factors in (4.13).

As a more advance example, consider

$$r = 1, \quad M = 4, \quad m_* = (m_1 = 2, m_2 = 1, m_3 = 0, m_4 = 0). \tag{4.14}$$

The number of vertices $v_I^{(\ell)}$ in V_L and the number of vertices u_a in V_R are

$$v_L = \sum_\ell m_\ell = 3, \quad v_R = Mr + 1 = 5. \tag{4.15}$$

There are 2 edges incident to the vertices $v_1^{(1)}$ and $v_2^{(1)}$ and 3 edges incident to the vertex $v_1^{(2)}$. An example of poles satisfying the Jeffrey–Kirwan rule is given by the choice of sine factors[16]

$$\sin(u_1 - v_1^{(1)} - \xi), \quad \sin(u_4 - v_1^{(1)} - \xi),$$
$$\sin(u_1 - v_2^{(1)} - \xi), \quad \sin(u_5 - v_2^{(1)} - \xi), \tag{4.16}$$
$$\sin(u_1 - v_1^{(2)} - \xi), \quad \sin(u_2 - v_1^{(2)} - \xi), \quad \sin(u_3 - v_1^{(2)} - \xi).$$

This choice corresponds to the bipartite graph in $\mathcal{G}(\vec{L}_{m_*,1})$ in Figure 10.

---

[16] As usual, $v_1^{(1)}$ is understood to be zero below, though we sometimes write it explicitly to make the notation more uniform.
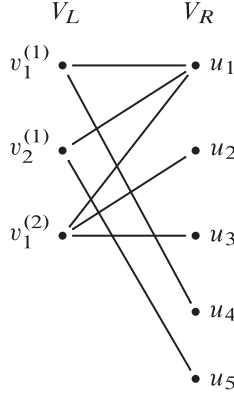
Figure 10. The bipartite graph corresponding to the pole in (4.16). In this example $M = 4$, $r = 1$, and the partition is $m_* = (2, 1, 0, 0)$. The number of vertices are $v_L = 3$ and $v_R = 5$. There are 2 edges incident to the vertices $v_1^{(1)}$ and $v_2^{(1)}$ and 3 edges incident to the vertex $v_1^{(2)}$.

4.4. From bipartite graphs to poles: the tree rule. So far we have translated every pole (modulo the degeneracy of choosing the flavor fugacities (4.11)) satisfying the Jeffrey–Kirwan rule into a bipartite graph in $\mathcal{G}(\vec{L}_{m_*,r})$. However not every bipartite graph in $\mathcal{G}(\vec{L}_{m_*,r})$ has an associated contributing pole in the index problem. As we argue in this section, only those $G \in \mathcal{G}(\vec{L}_{m_*,r})$ that are connected and have no cycles, known as *trees* in graph theory, correspond to poles that exist. This will be referred as the "Tree rule."

The essential logic may be demonstrated in a basic example. For instance, for $r = 1$, the candidate pole

$$\sin(u_1 - \xi_i^{(1,1)}), \quad \sin(u_1 - \xi_j^{(1,1)}), \tag{4.17}$$

for some $i \neq j$ corresponds to the bipartite graph in Figure 11(a). At this hypothetical pole we have $u_1 - \xi_i^{(1,1)} = 0$ and $u_1 - \xi_j^{(1,1)} = 0$. However, this implies a relation among the flavor fugacities and violates our choice of these parameters as generic complex numbers (4.1). Thus, there is in fact no pole associated to the choice of vanishing factors (4.17). The key observation is that the relation on the flavor fugacities arises from a cycle in the corresponding graph.

As a more advanced example with $r = 1$, consider the hypothetical choice of vanishing factors

$$\begin{aligned} \sin(u_1 - v_1^{(1)} - \xi_i^{(1,1)}), \quad \sin(u_2 - v_1^{(1)} - \xi_j^{(1,1)}), \\ \sin(u_1 - v_2^{(1)} - \xi_k^{(2,1)}), \quad \sin(u_2 - v_2^{(1)} - \xi_\ell^{(2,1)}). \end{aligned} \tag{4.18}$$

At this candidate pole one then has

$$u_1 - u_2 = \xi_i^{(1,1)} - \xi_j^{(1,1)} = \xi_k^{(2,1)} - \xi_\ell^{(2,1)},$$

which is again in contradiction with our generic choice of the flavor fugacities (4.1). Thus there is no such pole. Again we see that there is a cycle in the associated graph Figure 11(b).
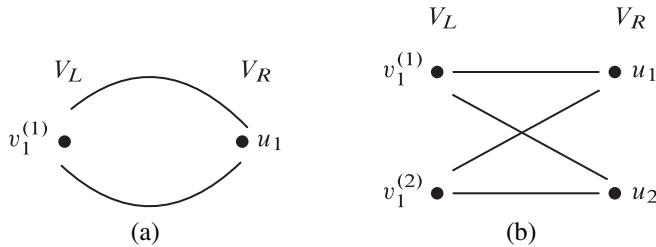
Figure 11. Two bipartite graphs corresponding to (4.17) and (4.18). They do not represent actual poles because they are not trees (connected graphs with no cycle).

The phenomenon illustrated in these examples is general. Any graph with a cycle does not correspond to an actual pole because the associated choice of vanishing factors implies a false relation on the flavor fugacities. Indeed, it is easy to construct such a relation by summing the arguments of the sine factors associated to the edges in the cycle with alternating signs.

In conclusion a pole exists and contributes to the index if and only if the associated bipartite graph $G \in \mathcal{G}(\vec{L}_{m_*,r})$ has no cycles. Since the number of edges is $e = v_L + v_R - 1$ an elementary result in graph theory (Proposition 1 in §5) then shows that the graph is in fact a tree *i.e.* a connected graph with no cycle. We have hence arrived at our Tree rule:

Tree rule. *A bipartite graph in $\mathcal{G}(\vec{L}_{m_*,r})$ corresponds to a pole if and only if it is a tree.*

This completes our graph theoretic enumeration of poles contributing to the residue formula (4.2). To determine the full y dependent index of the star quiver (and hence also the Kronecker quiver) we must sum the resulting contributions from each tree. We carry out this procedure in §6 for various examples.

In the case of the Euler characteristic, the results of this section provide more complete information. Given a star quiver associated to the partition m_* and a non-negative integer r, the number of contributing poles is the number of

trees in the set $\mathcal{G}(\vec{L}_{m_*,r})$, which we call $T(\vec{L}_{m_*,r})$. Each pole contributes to the Euler characteristic by $1/(Mr+1)!$. Combining these with the choices of flavor fugacities (4.11), we arrive at the formula

$$\chi(\mathcal{M}_{m_*,Mr+1}^k) = \frac{1}{(Mr+1)!} T(\vec{L}_{m_*,r}) \prod_{\ell=1}^{M} \left[\binom{\ell k}{\ell r + 1} (\ell r + 1)! \right]^{m_\ell}, \quad (4.19)$$

with $T(\vec{L}_{m_*,r})$ the number of trees with incidence data as described in §2.3.

5. Graph theory

In this section we will prove the tree counting Theorem 1 in graph theory language. Combined with the results of §4, this completes the derivation of our main result (2.28) for the Euler characteristic of Kronecker moduli space.

In §5.1 we introduce necessary basic notions in graph theory. In §5.2 we define the concept of *division* of a bipartite graph which crucial to our proof. Finally, in §5.3 we prove the tree counting theorem using divisions.

5.1. Generalities in graph theory. We begin with a review of various basic notions in graph theory. We denote the number of vertices and edges of a graph G by v and e, respectively. All the graphs of interest are *undirected* graphs (the edges are unorientated).

Definition 1. Let G be a graph consisting of vertices and edges. A *trail* is a sequence of vertices and edges in G, where each edge's endpoints are the preceding and following vertices in the sequence. A *path* is a trail where no vertices (and hence edges) are repeated, except possibly the first and the last. A *cycle* is a path in which the first and the last vertices are the same.

Definition 2. Let G be a graph. G is a *tree* if it is connected and has no cycle.

Proposition 1. *The following are equivalent for a graph G with e edges and v vertices*:

- *G is a tree*;
- *G is connected and $e = v - 1$*;
- *G has no cycle and $e = v - 1$*.

Proof. See, for example, Theorem 3.1.3 of [46].   □

The graphs of most interest for our purpose are bipartite graphs:

Definition 3. A *bipartite graph* is a graph whose vertices can be divided into two disjoint sets V_L and V_R such that every edge connects a vertex in V_L to V_R. V_L and V_R are called the *partite sets*.

We denote a bipartite graph by $G = (V_L + V_R, E)$ with E being the set of edges in the graph. We denote the number of vertices in V_L and V_R by v_L and v_R, respectively. As before, the total number of vertices and edges are indicated by $v(= v_L + v_R)$ and e, respectively.

5.2. Division of bipartite graphs. In this section we develop various concepts which are useful preliminaries to the tree counting Theorem 1. The main idea is called division defined below.

Definition 4 (Division). Let $G = (V_L + V_R, E)$ be a bipartite graph. A *division* of G is a disjoint union $E = L \cup R$ of edges such that the following conditions hold:

- each vertex in V_L is incident to at most one edge in L (blue);

- each vertex in V_R is incident to at most one edge in R (red).

Each of L and R will be called a *compartment* of the division. We will put the edges in L and R in blue and red, respectively. G is said to be *divisible* if it admits a division.

Remark 1. Not every bipartite graph is divisible. See Figure 12 for a simple example.
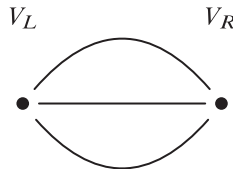
Figure 12. A bipartite graph that is not divisible. If it were divisible, then two of the three edges must belong to the same compartment, say, L. This leads to a contradiction because the vertex in V_L is incident to two edges in L.
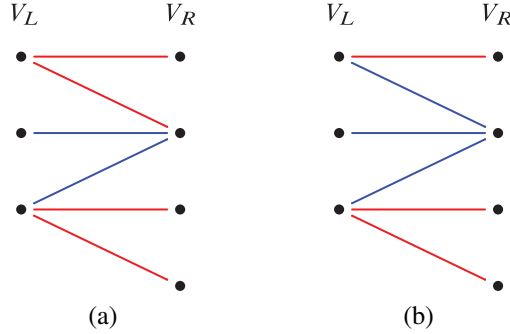
Figure 13. (a) An example of a division, where each vertex in V_L is incident to *at most* one edge in L (blue) while each vertex in V_R is incident to *at most* one edge in R (red). (b) An example of a left maximal division of the same bipartite graph. In a left maximal division every vertex in V_L is incident to *exactly one* edge in the compartment L (blue).

Remark 2. Let the numbers of edges in L and R be e_L and e_R, respectively. Clearly, e_L (e_R resp.) cannot be bigger than v_L (v_R resp.).

Definition 5 (maximal division). A division $E = L \cup R$ of $G = (V_L + V_R, E)$ is said to be *left maximal* if each vertex in V_L is incident to exactly one edge in L, i.e. $e_L = v_L$. Similarly for the *right maximal* division.

Proposition 2. *Let G be a bipartite tree. Then there is no division of G that is simultaneously left and right maximal.*

Proof. Suppose there is a simultaneous left and right maximal division of bipartite tree G, then $e_L = v_L$ and $e_R = v_R$. The total number of edges is

$$e = e_L + e_R, \tag{5.1}$$

which is equal to the total number of vertices $v_L + v_R$. By Proposition 1, G cannot be a tree, hence a contradiction. □

Theorem 2. *Let $G = (V_L + V_R, E)$ be a bipartite tree. Then G has exactly v_R left maximal divisions.*

Proof. We will prove this by explicit constructions of the v_R left maximal divisions, each of which corresponds to a vertex in V_R.

Pick a vertex v in V_R. Let the edges incident to v be $\{e^{(1)}, e^{(2)}, \ldots, e^{(Q)}\}$ for some positive integer Q. For each edge $e^{(i)}$, we will construct a subgraph $T_v^{(i)}$ equipped with a left maximal division by the following algorithm. First, color the

edge $e^{(i)}$ in blue, *i.e.* assign the edge $e^{(i)}$ to the compartment L. Denote the other endpoint of $e^{(i)}$ by $v_1^{(i)}$. Since $v_1^{(i)}$ is already incident to a blue edge (*i.e.* an edge in L), the remaining edges, if any, that are incident to $v_1^{(i)}$ must be in red (*i.e.* belonging to R). Let us denote these red edges by $e_1'^{(i)}, \dots, e_n'^{(i)}$ and the vertices in V_R they are incident to by $v_1'^{(i)}, v_2'^{(i)}, \dots, v_n'^{(i)}$. Now for each of the vertices $v_j'^{(i)}$ in V_R, since it is already incident to a red edge $e_j'^{(i)}$, the remaining edges, if any, that are incident to $v_j'^{(i)}$ must be in blue. We repeat this argument and continue the construction till the point when every terminal vertex is incident to only one edge. In this way, for each edge $e^{(i)}$ incident to v, we have constructed a subtree $T_v^{(i)}$ equipped with a left maximal division.

Let us note the following two properties of the subtree $T_v^{(i)}$.

- First, the intersection of two different subtrees $T_v^{(i)}$ consists only of the original vertex v,

$$T_v^{(i)} \cap T_v^{(j)} = \{v\}, \quad i \neq j. \tag{5.2}$$

  Suppose not, then there is another vertex $v' \in T_v^{(i)} \cap T_v^{(j)}$ and $v' \neq v$. We can then form a cycle passing through v and v' in the union $T_v^{(i)} \cup T_v^{(j)}$, hence contradicting the fact that G has no cycle.

- Second, the union of $T_v^{(i)}$ covers the whole graph G,

$$G = \bigcup_i T_v^{(i)}, \quad \text{for all } v \in V_R. \tag{5.3}$$

  This follows from the fact that G is assumed to be connected, so there is a path between v and any other point. This path must belong to one of the subtrees $T_v^{(i)}$ by construction.

Combining the above two properties, we see that for each vertex $v \in V_R$, we can construct a left maximal division of G inherited from that of $T_v^{(i)}$. We will denote this left maximal division of G by $E = L_v \cup R_v$. Note that in $E = L_v \cup R_v$, v is the unique vertex in V_R that is connected to only blue lines, while each of the other $v_R - 1$ vertices is incident to exactly one red line. We illustrate this algorithm for two different vertices in the same bipartite graph in Figure 14 and 15.

Next, we want to show that there are no other left maximal divisions of G than $E = L_v \cup R_v$. Let us note that the number of blue lines e_L in a left maximal division is the number of vertices in V_L, $e_L = v_L$ by definition. By Proposition 1, the number of edges e in a tree is $v_L + v_R - 1$. Hence the number of red lines e_R in a left maximal division of a tree is

$$e_R = e - e_L = (v_L + v_R - 1) - v_L = v_R - 1. \tag{5.4}$$

Since every vertex in V_R is allowed to incident to at most one red line, it follows that among the v_R vertices in V_R, there is exactly one of them, say, v, that is incident to only blue lines. The colors of the remaining edges are thus determined by the algorithm above to be those of $E = L_v \cup R_v$, and hence there are no left maximal divisions other than $E = L_v \cup R_v$ for $v \in V_R$. $\square$
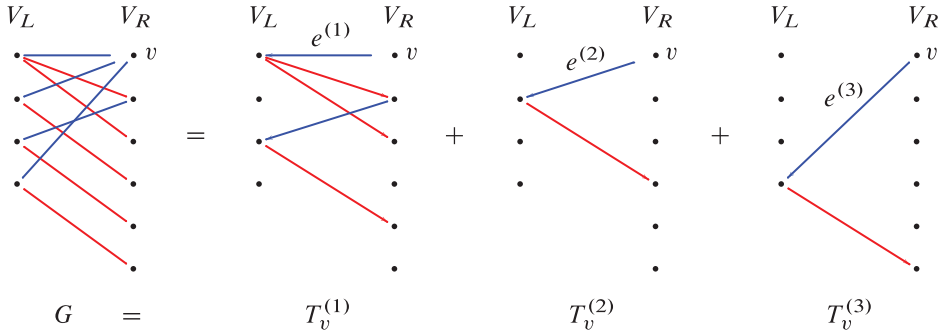
Figure 14. Construction of a left maximal division associated to the vertex v of a tree G. The graph G is further decomposed into the union of 3 subtrees $T_v^{(i)}$, each of which is associated to an edge $e^{(i)}$ incident to the original vertex v. v is the only vertex in V_R that is incident to only blue lines. In a left maximal division, each vertex in V_L is incident to *exactly one* blue line, while each vertex in V_R is incident to *at most* one red line. In addition to the above left maximal division, there are in total 6 left maximal divisions of G, each of which is associated to a vertex in V_R. The orientations on the edges indicate the order of the steps in the algorithm. The graph itself is still undirected.
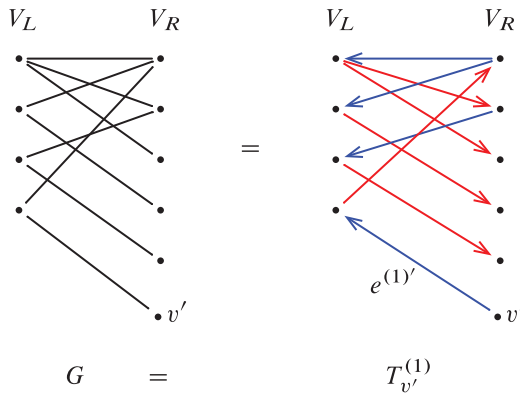
Figure 15. Construction of a left maximal division associated to the vertex v' of a tree G. In this case the decomposition of G is trivial, $G = T_{v'}^{(1)}$. In a left maximal division, each vertex in V_L is incident to *exactly one* blue line, while each vertex in V_R is incident to *at most* one red line. The orientations on the edges indicate the order of the steps in the algorithm. The graph itself is still undirected.

In summary, we have shown that the v_R left maximal divisions $E = L_v \cup R_v$ constructed above are the only left maximal divisions for a tree G. In the division $E = L_v \cup R_v$, v is the unique vertex in V_R that is connected to only blue lines, while each of the other $v_R - 1$ vertices is incident to exactly one red line. The tree G can be decomposed into unions of smaller trees, $G = \bigcup_i T_v^{(i)}$. Each subtree $T_v^{(i)}$ grows from an edge $e^{(i)}$ incident to v. The intersection of two different trees $T_v^{(i)}$ is always the original vertex, $T_v^{(i)} \cap T_v^{(j)} = \{v\}$ for $i \neq j$.
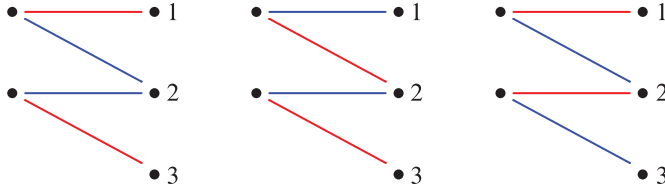
Figure 16. The 3 left maximal divisions of an tree bipartite graph in $\mathcal{G}(\vec{L})$, where $\vec{L} = (1,1) \, (= \vec{L}_{(m_1=2, m_2=0), 1})$. A bipartite graph in $\mathcal{G}(\vec{L})$ has $v_L = 2$ vertices in V_L and $v_R = 3$ vertices in V_R, with a total number of $e = 4$ edges. In a division, each vertex in V_L is incident to at most one edge in L (blue) and each vertex in V_R is incident to at most one edge in R (red). In the case of left maximal division, each vertex in V_L is incident to exactly one blue edge in L.

5.3. Proof of the tree counting theorem.
In this section we prove the tree counting theorem (2.21). From the proof of Theorem 2, we have learned how to construct left maximal divisions for a given bipartite tree graph $G = (V_L + V_R, E)$. We now reverse the logic to prove the tree counting theorem: we enumerate the total number of left maximal divisions of trees in $\mathcal{G}(\vec{L})$ and then divide by the degeneracy v_R to obtain the number of (uncolored) bipartite tree graphs.

Let us recall the incidence data defining the set of bipartite graphs $\mathcal{G}(\vec{L})$ from a v_L component vector $\vec{L}$ with non-negative integral components.

- There are v_L vertices in V_L.
- There are $v_R = 1 + \sum_{i=1}^{v_L} L_i$ vertices in V_R.
- There are $L_i + 1$ edges incident to the i-th vertex in V_L.

For a tree G in $\mathcal{G}(\vec{L})$, the number of edges e_L and e_R in the compartment L (blue) and R (red) in a left maximal division $E = L_v \cup R_v$ of G is

$$e_L = v_L, \quad e_R = \sum_{i=1}^{v_L} L_i. \tag{5.5}$$

The i-th vertex in V_L is incident to exactly one blue line (being left maximal) and L_i red lines.

Strategy of the Proof. We now enumerate left maximal divisions in $\mathcal{G}(\vec{L})$ that are trees and thereby obtain the number of (uncolored) trees. The procedure is outlined below:

- **Step 1.** Draw L_i red lines from the i-th vertex in V_L. Connect the $\sum_i L_i$ red lines to vertices in V_R, with each one of them incident to *at most* one red line. We refer to the resulting graph as the *red graph*.

- **Step 2.** Draw exactly one blue line from each vertex in V_L. Connect the v_L blue lines to vertices in V_R such that the whole graph is connected. Up to this step we have constructed a left maximal division of a tree in $\mathcal{G}(\vec{L})$.

- **Step 3.** Consider all the left maximal divisions constructed above. Identify those left maximal divisions that correspond to the same (uncolored) tree. Divide the number of connected left maximal divisions by this degeneracy to get $T(\vec{L})$.

Note that by Proposition 1, in the case of $e = v_L + v_R - 1$, a graph is connected if and only if it has no cycles. Therefore, in order to enumerate the trees, it suffices to ensure the connectivity of the graph. Also note that we never generate cycles at Step 1, so it suffices to impose the connectivity condition at Step 2.

Given a red graph G_R constructed in Step 1, let the number of *connected* left maximal divisions in $\mathcal{G}(\vec{L})$ that contain G_R be $B(\vec{L})$. Clearly $B(\vec{L})$ does not depend on the choice of the red graph G_R because every red graph has the same topology. We have the following lemma:

Lemma 1. *Given a red graph G_R constructed in Step 1, the number of connected left maximal divisions in $\mathcal{G}(\vec{L})$ that contain G_R is*

$$B(\vec{L}) = v_R^{v_L - 1}, \tag{5.6}$$

where $v_R = 1 + \sum_{i=1}^{v_L} L_i$. In particular, $B(\vec{L})$ does not depend on the choice of the red graph G_R.

Before proving this lemma, let us note that we are now ready to prove Theorem 1.

Proof of the tree counting theorem. Starting from Step 1, there are $e_R = \sum_i L_i$ red lines whereas there are $v_R = 1 + \sum_i L_i$ vertices in V_R, each of which is allowed to be incident to *at most* one red line. It follows that exactly one vertex in V_R has no red line incident to it. Hence, the number of red graphs constructed in

Step 1 is

$$v_R \frac{(v_R - 1)!}{\prod_{i=1}^{v_L} L_i!},\tag{5.7}$$

where v_R comes from choosing which vertex in V_R is left out and the multinomial coefficient $\frac{(v_R-1)!}{\prod_{i=1}^{v_L} L_i!}$ comes from permuting the $v_R - 1$ red lines.

Next for Step 2, Lemma 1 instructs us to multiply the counting by a factor of $B(\vec{L}) = v_R^{v_L - 1}$.

Finally for Step 3 we divide the counting by the degeneracy of left maximal divisions for a given tree $G \in \mathcal{G}(\vec{L})$, which is simply v_R by Theorem 2.

Combining all these factors together, we have

$$T(\vec{L}) = \underbrace{v_R \frac{(v_R - 1)!}{\prod_{i=1}^{v_L} L_i!}}_{\text{Step 1}} \times \underbrace{v_R^{v_L - 1}}_{\text{Step 2}} \times \underbrace{\frac{1}{v_R}}_{\text{Step 3}},\tag{5.8}$$

where the red (blue) factors are the number of ways to draw the red (blue) lines. Hence we have proved the tree counting Theorem 1. □

Thus, to complete the argument, it remains to prove Lemma 1.

Proof of Lemma 1. It suffices to show the following claim. Let v be a positive integer. Let $L_{0a}, L_{0b}, L_1, L_2, \ldots, L_{v-1}$ be some non-negative integers. Let $\mathcal{I}$ be the index set $\mathcal{I} = \{0a, 0b, 1, 2, \ldots, v-1\}$. Define

$$\vec{L}^{(1)} = \underbrace{(L_{0a} + L_{0b}, L_1, \ldots, L_{v-1})}_{v},\tag{5.9}$$

$$\vec{L}^{(2)} = \underbrace{(L_{0a}, L_{0b}, L_1, \ldots, L_{v-1})}_{v+1}.\tag{5.10}$$

We will denote the sets of vertices on the left for graphs in $\mathcal{G}(\vec{L}^{(1)})$ and $\mathcal{G}(\vec{L}^{(2)})$ by $V_L^{(1)}$ and $V_L^{(2)}$, respectively. The number of vertices in $V_L^{(1)}$ and $V_L^{(2)}$ are respectively

$$v_L^{(1)} = v, \quad v_L^{(2)} = v + 1.\tag{5.11}$$

The number of vertices on the right in $\mathcal{G}(\vec{L}^{(1)})$ and $\mathcal{G}(\vec{L}^{(2)})$ are both

$$v_R = 1 + \sum_{i \in \mathcal{I}} L_i.\tag{5.12}$$

We will therefore denote the sets of vertices on the right in $\mathcal{G}(\vec{L}^{(1)})$ and $\mathcal{G}(\vec{L}^{(2)})$ by the same symbol V_R without superscripts. See Figure 17 for examples of tree in $\mathcal{G}(\vec{L}_1)$ and $\mathcal{G}(\vec{L}_2)$.

Claim. $B(\vec{L}^{(2)}) = v_R \, B(\vec{L}^{(1)})$.

Observe that this claim suffices to prove the lemma. Indeed for any $\vec{L}$ we have $B(\vec{L}) = 1$ for[17] $v_L = 1$. Thus, Lemma 1 follows immediately from the above claim by induction on v_L.

Proof of the claim. Let us label the vertices in V_R by $1, 2, \ldots, v_R = 1 + \sum_{i \in \mathcal{J}} L_i$,

$$V_R = \{1, 2, \ldots, v_R\}. \tag{5.13}$$

For reasons that will become clear momentarily, we will label the vertices in $V_L^{(1)}$ and $V_L^{(2)}$ as

$$V_L^{(1)} = \{0, 1, 2, \ldots, v - 1\}, \tag{5.14}$$

$$V_L^{(2)} = \{0a, 0b, 1, 2, \ldots, v - 1\}. \tag{5.15}$$

Since $B(\vec{L})$ does not depend on the choice of the red graph, we will pick a convenient red graph $G_R^{(1)}$ in $\mathcal{G}(\vec{L}^{(1)})$ such that the first $L_{0a} + L_{0b}$ vertices in V_R are incident to the vertex 0 in $V_L^{(1)}$, the next L_1 vertices in V_R are incident to the vertex 1 in $V_L^{(1)}$ and so on. Similarly, we will pick a convenient red graph $G_R^{(2)}$ in $\mathcal{G}(\vec{L}^{(2)})$ such that the first L_{0a} vertices in V_R are incident to the vertex $0a$ in $V_L^{(2)}$, the next L_{0b} vertices in V_R are incident to the vertex $0b$ in $V_L^{(2)}$ and so on. The last vertex in V_R is left out in both $G_R^{(1)}$ and $G_R^{(2)}$. Let $S_a \subseteq V_R$ be the set of the first L_{0a} vertices in V_R and $S_b \subseteq V_R$ be the next L_{0b} vertices in V_R.

We will denote the set of *connected* (and therefore tree in this case) left maximal divisions in $\mathcal{G}(\vec{L}^{(I)})$ that contain $G_R^{(I)}$ as $\mathcal{B}(\vec{L}^{(I)})$, with $I = 1, 2$. The number of graphs in $\mathcal{B}(\vec{L}^{(I)})$ is by definition $B(\vec{L}^{(I)})$. We will label a graph $b^{(1)}$ in $\mathcal{B}(\vec{L}^{(1)})$ by a tuple of v positive integers as

$$b^{(1)} = (n_0, n_1, \ldots, n_{v-1}) \in \mathcal{B}(\vec{L}^{(1)}), \tag{5.16}$$

meaning the vertex i in $V_L^{(1)}$ is incident to the vertex n_i in V_R by a blue line.

---

[17] For $v_L = 1$, the vector has only one component, $\vec{L} = (L_1)$. We can choose a red graph in Step 1 to be that each of the first L_1 vertices in V_R is incident to a red line while the last vertex is left out. In order not to have a cycle, the blue line has to be incident to the last vertex in V_R, and hence $B(\vec{L}) = 1$.

Together with the fact that $b^{(1)}$ contains the red graph $G_R^{(1)}$, this tuple of integers uniquely determines the left maximal division $b^{(1)}$. Similarly we label a graph $b^{(2)}$ in $\mathcal{B}(\vec{L}^{(2)})$ by a tuple of $\nu + 1$ positive integers as

$$b^{(2)} = (N_{0a}, N_{0b}, N_1, \ldots, N_{\nu-1}) \in \mathcal{B}(\vec{L}^{(2)}). \tag{5.17}$$

Note that not every choice of integers correspond to a connected graph, and therefore does not belong to $\mathcal{B}(\vec{L}^{(1)})$. For example, we have

$$N_{0a} \notin S_a, \quad \text{if } b^{(2)} \in \mathcal{B}(\vec{L}^{(2)}). \tag{5.18}$$

And similarly $N_{0b} \notin S_b$ if $b^{(2)} \in \mathcal{B}(\vec{L}^{(2)})$. Otherwise we can form a cycle using the corresponding blue line and a red line in $G_R^{(2)}$. Also, graphs with $N_{0a} \in S_b$, and $N_{0b} \in S_a$ have a cycle. We therefore have

$$N_{0a} \notin S_b \quad \text{or} \quad N_{0b} \notin S_a, \quad \text{if } b^{(2)} \in \mathcal{B}(\vec{L}^{(2)}). \tag{5.19}$$

For the same reason we have

$$n_0 \notin S_a \cup S_b, \quad \text{if } b^{(1)} \in \mathcal{B}(\vec{L}^{(1)}). \tag{5.20}$$

These requirements will be important in the following.

Now define the *merging map*

$$\mu \colon \mathcal{B}(\vec{L}^{(2)}) \longrightarrow \mathcal{B}(\vec{L}^{(1)})$$

as

$$\mu \colon (N_{0a}, N_{0b}, N_1, \ldots, N_{\nu-1})$$
$$\longmapsto \begin{cases} (n_0 = N_{0a}, n_1 = N_1, \ldots, n_{\nu-1} = N_{\nu-1}) & \text{if } N_{0a} \notin S_b, \\ (n_0 = N_{0b}, n_1 = N_1, \ldots, n_{\nu-1} = N_{\nu-1}) & \text{if } N_{0a} \in S_b. \end{cases} \tag{5.21}$$

See Figure 17 for examples of the merging map.

We need to make sure the merging map is consistent with (5.18), (5.19), and (5.20). First note that N_{0a} is never in S_a for $b^{(2)} \in \mathcal{B}(\vec{L}^{(2)})$ by (5.18), so we do not have to worry about hitting a point with $n_0 = N_{0a} \in S_a$, which does not belong $\mathcal{B}(\vec{L}^{(1)})$ by (5.20). Secondly, in the case when $N_{0a} \in S_b$, from (5.19) it follows that $N_{0b} \notin S_a$. From (5.18) we know $N_{0b} \notin S_b$. Hence $N_{0b} \notin S_a \cup S_b$ if $N_{0a} \in S_b$. It follows that the image graph $(n_0 = N_{0b}, n_1 = N_1, \ldots, n_{\nu-1} = N_{\nu-1})$ lies in $\mathcal{B}(\vec{L}^{(1)})$.
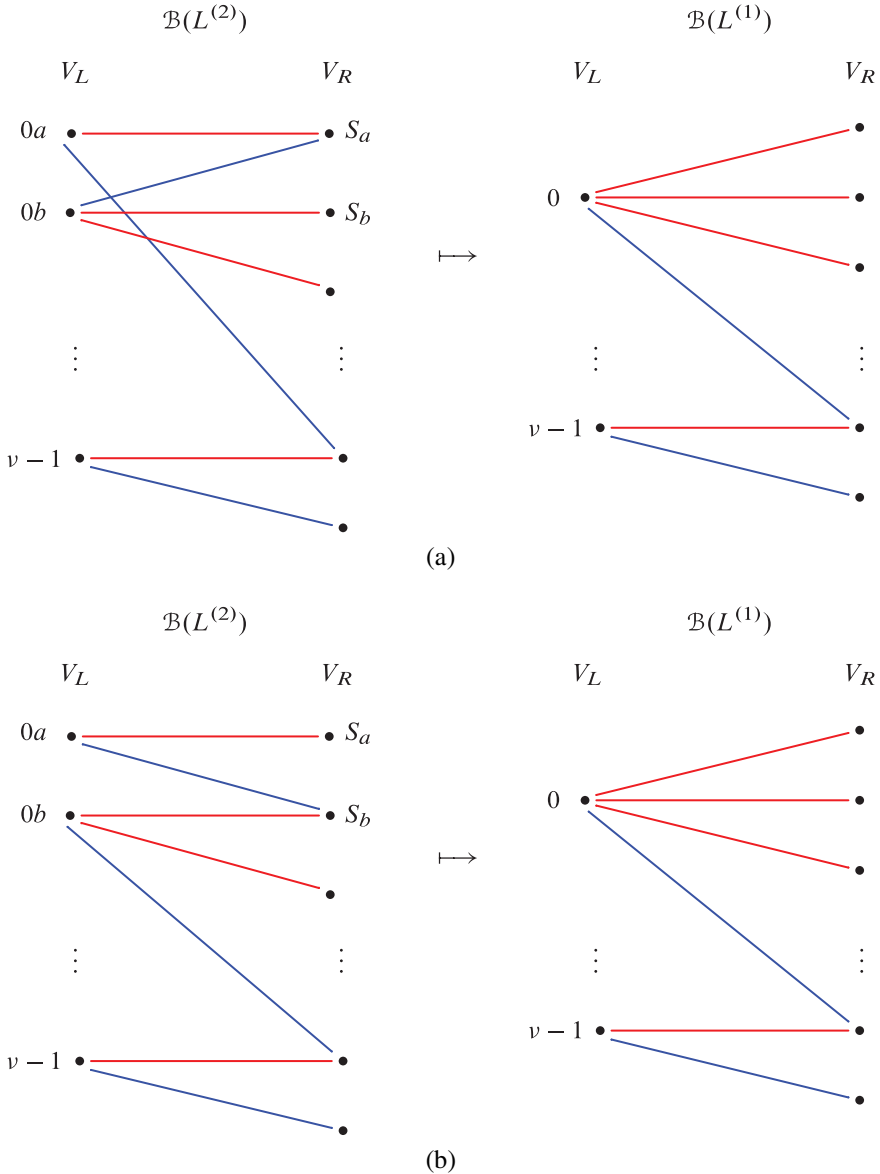
Figure 17. An illustration of the merging map $\mu \colon \mathcal{B}(L^{(2)}) \to \mathcal{B}(L^{(1)})$. In this example $L_{0a} = 1$ and $L_{0b} = 2$. S_a only contains the first vertex in V_R while S_b consists of the second and third vertices in V_R. (a) The case $N_{0a} \notin S_b$. (b) The case $N_{0a} \in S_b$.

It is clear that the merging map μ is surjective. We now argue that μ is v_R-to-1. This then proves the claim.

Thus, fix a graph $b^{(1)} = (n_0, n_1, \ldots, n_{v-1})$, we wish to show that its preimage consists of exactly v_R graphs. Let $b^{(2)} = (N_{0a}, N_{0b}, N_1, \ldots, N_{v-1}) \in \mathcal{B}(\vec{L}^{(2)})$ such that $\mu(b^{(2)}) = b^{(1)}$.

If $N_{0a} \notin S_b$, then N_{0a} is fixed to be n_0 for $\mu(b^{(2)}) = b^{(1)}$, while we can freely choose $N_{0b} \in V_R - S_b$. There are $v_R - L_{0b}$ graphs in the preimage of this kind. On the other hand, if $N_{0a} \in S_b$, then N_{0b} is fixed to be n_0 for $\mu(b^{(2)}) = b^{(1)}$, while we can freely choose N_{0a} to be any point in S_b. There are L_{0b} graphs in the preimage of this kind. Hence, given any graph $b^{(1)} \in \mathcal{B}(\vec{L}^{(1)})$, we have shown that there are v_R graphs in the preimage $\mu^{-1}(b^{(1)})$. $\qquad\square$

6. Computations of the refined index

Thus far in this work we have primarily been concerned with the degeneracy $\Omega(M, N, k)$. In this section, we extend our analysis to the full y-dependent index $\Omega(M, N, k, y)$ whose definition we recall here

$$\Omega(M, N, k, y) \equiv \sum_{p=0}^{d} y^{2p-d} \, h^{p,p}(\mathcal{M}_{M,N}^{k}), \tag{6.1}$$

where d is the complex dimension of the moduli space

$$d = kMN - M^2 - N^2 + 1. \tag{6.2}$$

The y-dependent index contains much more information than the simple degeneracy $\Omega(M, N, k)$. As a consequence, it is more challenging to determine. Nevertheless as we will see, the residue technique described in detail in §4 can be extended to a useful algorithm for computing the full index $\Omega(M, N, k, y)$. We present explicit formulas for small M and N in equation (6.30).

To begin the analysis, we first note that the MPS degeneration formula can be generalized to include the full y dependence of the index [40]. In the case of the Kronecker quiver with dimension vector (M, N), if we apply the MPS degeneration formula on the node M, we have

$$\Omega(M, N, k, y) = y^{-M(M-1)-d} \sum_{m_* \vdash M} \Big[\prod_{\ell=1}^{M} \frac{1}{m_\ell!} \Big(\frac{(-1)^{\ell-1}}{\ell [\ell]_{y^2}} \Big)^{m_\ell} \Big] y^{d_{m_*}} \Omega(\mathcal{M}_{m_*,N}^{k}, y),$$

$$\tag{6.3}$$

where

$$[n]_q = \frac{1 - q^n}{1 - q},$$ (6.4)

and d_{m_*} is the complex dimension of the moduli space for the star quiver associated to the partition $m_* \vdash M$,

$$d_{m_*} = kMN - \sum_{\ell=1}^{M} m_\ell - N^2 + 1.$$ (6.5)

Thus, to compute the refined index $\Omega(M, N, k, y)$, it suffices to determine the refined indices of star quivers $\Omega(\mathcal{M}^k_{m_*,N}, y)$. This can be carried out with the residue formula of §4. As described there, contributing poles in the residue formula correspond to bipartite trees. Each pole comes with an associated y-dependent contribution which we sum to determine the refined index.

In the remainder of this section, we apply the formula to the Kronecker quiver with dimension vector $(2, 2r + 1)$ with k arrows.
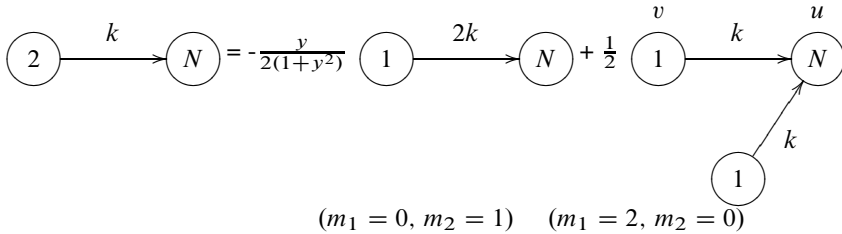
Figure 18. An example of the MPS degeneration formula for $M = 2$. The first and the second quiver on the righthand side correspond to the partition $(m_1 = 0, m_2 = 1)$ and $(m_1 = 2, m_2 = 0)$ of $M = 2$, respectively.

6.1. Example: $(2, 1)$. As a gentle warmup to the more detailed calculations that follow, we begin with the case $r = 0$ and dimension vector $(2, 1)$. As discussed in §2.1.1, the moduli space is the Grassmannian $\mathrm{Gr}(2, k)$ and we aim to reproduce the associated index (2.12).

There are two partitions

$$m_*^{(1)} = (m_1 = 0, m_2 = 1) \quad \text{and} \quad m_*^{(2)} = (m_1 = 2, m_2 = 0)$$

appearing in the degeneration formula (6.3) (see Figure 18). The quiver moduli space for the first partition is $\mathbb{CP}^{2k-1}$ and we have

$$
\begin{aligned}
\Omega(\mathcal{M}^k_{m_*^{(1)},1}, y) &= y^{-2k+1} + y^{-2k+3} + \cdots + y^{2k-3} + y^{2k-1} \\
&= y^{-2k+1}[2k]_{y^2}.
\end{aligned}
\tag{6.6}
$$

For the second partition $m_*^{(2)}$ in Figure 18, the integrand for the residue formula is given by the general formula (4.4):[18]

$$
\left(\frac{1}{\sin z}\right)^2 \prod_{i=1}^k \frac{\sin(u - \xi_i^{(1)} + z)}{\sin(u - \xi_i^{(1)})} \frac{\sin(u - v - \xi_i^{(2)} + z)}{\sin(u - v - \xi_i^{(2)})},
\tag{6.7}
$$

where u, v stand for the gauge fugacities for the rightmost and the leftmost node in the three-node quiver of Figure 18. We also recall that z is defined by $y = e^{iz}$. The remaining node is decoupled. Meanwhile, $\xi^{(1)}$ and $\xi^{(2)}$ are the SU(k) flavor fugacities for the lower and upper group of arrows in Figure 18, respectively. From the analysis in §4, we see that the Jeffrey–Kirwan rule instructs us to pick up one factor of $\sin(u - \xi_i^{(1)})$ and one factor of $\sin(u - v - \xi_i^{(2)})$, and then sum over the contributions from all such choices.

In the language of bipartite graphs, this set of poles corresponds to a single tree in $\mathcal{G}(\vec{L}_{m_*^{(2)},0})$. Recall that a bipartite graph $G \in \mathcal{G}(\vec{L}_{m_*^{(2)},0})$ has[19]

$$
v_L = \sum_\ell m_\ell = 2, \quad v_R = Mr + 1 = 1, \quad e = Mr + \sum_\ell m_\ell = 2,
\tag{6.8}
$$

where v_L and v_R are the number of vertices in V_L and V_R and e is the total number of edges in G. The 2-dimensional vector is $\vec{L}_{m_*^{(2)},0} = (0,0)$. Each vertex in V_L is incident to 1 edge. The number of trees in $\mathcal{G}(\vec{L}_{m_*^{(2)},0})$ is given by the tree counting theorem (2.24)

$$
T(\vec{L}_{m_*^{(2)},0}) = 1.
\tag{6.9}
$$

This unique tree is illustrated in Figure 19.

---

[18] Here we use a slightly simplified convention on the superscripts for the gauge fugacity v and flavor fugacities ξ's compared with §4. To match the two conventions, we have $v_2^{(1)} = v$, $\xi_i^{(I=1,\ell=1)} = \xi^{(1)}$, and $\xi_i^{(2,1)} = \xi^{(2)}$.

[19] $M = 2$ and $r = 0$ here.
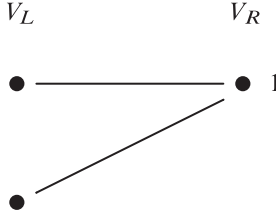
Figure 19. The only tree in $\mathcal{G}(\vec{L}_{m_*^{(2)},0})$, where the vector $\vec{L}_{m_*^{(2)},0} = (0,0)$. In this example, $M = 2$, $r = 0$, and $m_* = (m_1 = 2, m_2 = 0)$. The number of vertices in V_L and V_R are $v_L = 2$ and $v_R = 1$. The number of edges is $e = 2$. Each vertex in V_L is incident to 1 edge. There is a unique tree in $\mathcal{G}(\vec{L}_{m_*^{(2)},0})$ corresponding to the poles $u - \xi_i^{(1)} = 0$, $u - v - \xi_j^{(2)} = 0$ for different ξ's.

We now sum over these poles with different choices of ξ. The resulting expression is compactly stated in terms of variables $\xi_{mi}^{(I)} = \xi_m^{(I)} - \xi_i^{(I)}$ and the function

$$f(x) \equiv \frac{\sin(x + z)}{\sin(x)}. \tag{6.10}$$

We find

$$\Omega(\mathcal{M}_{m_*^{(2)},1}^k, y) = \sum_{m,n=1}^{k} \prod_{i=1, i\neq m}^{k} f(\xi_{mi}^{(1)}) \prod_{\ell=1, \ell\neq n}^{k} f(\xi_{n\ell}^{(2)}). \tag{6.11}$$

Despite its appearance, the index (6.11) is in fact independent of the flavor fugacities ξ due to $\mathcal{N} = 4$ supersymmetry [12]. We can therefore evaluate $\Omega(\mathcal{M}_{m_*^{(2)},1}^k, y)$ in a particular limit of ξ's and obtain the exact answer as a function of y (or equivalently, z). We choose the ξ's to be purely imaginary

$$\xi_m^{(I)} \in -i\mathbb{R}_+, \quad I = 1, 2, \tag{6.12}$$

and further order them so that

$$\begin{aligned} i\xi_1^{(I)} &\gg i\xi_2^{(I)} \gg \cdots \gg i\xi_k^{(I)} \gg 1, \quad I = 1, 2, \\ i\xi_{mm'}^{(1)} &\gg i\xi_{nn'}^{(2)}, \quad \text{for all } l, m < m', n < n'. \end{aligned} \tag{6.13}$$

In this limit we can replace the function $f(x)$ by the simpler expression

$$f(\xi_{mm'}^{(I)}) = \frac{\sin(\xi_{mm'}^{(I)} + z)}{\sin(\xi_{mm'}^{(I)})} \longrightarrow y^{\theta(m-m')} = \begin{cases} y & \text{if } m < m', \\ y^{-1} & \text{if } m > m', \end{cases} \tag{6.14}$$

where $\theta(x)$ is the step function,

$$\theta(x) = \begin{cases} +1 & \text{if } x > 0, \\ -1 & \text{if } x < 0. \end{cases} \tag{6.15}$$

In this limit we therefore have

$$\sum_{m=1}^{k} \prod_{i=1, i \neq m}^{k} f(\xi_{mi}^{(I)}) = y^{-(k-1)} + y^{-(k-3)} + \cdots + y^{k-1} \tag{6.16}$$
$$= y^{-(k-1)}[k]_{y^2}.$$

In fact, one can check that this trigonometric identity is true for arbitrary ξ's. It follows that the refined index for the star quiver associated to the second partition $m_*^{(2)}$ is

$$\Omega(\mathcal{M}_{m_*^{(2)},1}^k, y) = (y^{-(k-1)}[k]_{y^2})^2. \tag{6.17}$$

Assembling the pieces using the degeneration formula (6.3), we find that the refined index for the Kronecker quiver with dimension vector $(2, 1)$ and k arrows is

$$\Omega(2, 1, k, y) = y^{-2k+2} \Big(-\frac{1}{2[2]_{y^2}} y^{2k-1} \Omega(\mathcal{M}_{m_*^{(1)},1}^k, y) + \frac{1}{2} y^{2k-2} \Omega(\mathcal{M}_{m_*^{(2)},1}^k, y) \Big)$$

$$= \frac{y^{2(2-k)} \prod_{i=1}^{k}(1 - y^{2i})}{\prod_{i=1}^{2}(1 - y^{2i}) \prod_{i=1}^{k-2}(1 - y^{2i})}. \tag{6.18}$$

This is indeed the expected answer (2.12) for the Grassmannian[20] $\text{Gr}(2, k)$.

6.2. Example: $(2, 2r + 1)$. We now generalize the calculations of the previous example to compute the refined index for the Kronecker quiver with dimension vector $(2, 2r + 1)$ and k arrows.

The index for the first partition $m_*^{(1)} = (m_1 = 0, m_2 = 1)$ in Figure 18 is that for the Grassmannian $\text{Gr}(2r + 1, 2k)$,

$$\Omega(\mathcal{M}_{m_*^{(1)},2r+1}^k, y) = y^{-(2r+1)(2k-2r-1)} \frac{\prod_{i=1}^{2k}(1 - y^{2i})}{\prod_{i=1}^{2r+1}(1 - y^{2i}) \prod_{i=1}^{2k-(2r+1)}(1 - y^{2i})}, \tag{6.19}$$

if $2k \geq 2r + 1$ and zero otherwise. Note the exponent $(2r + 1)(2k - 2r - 1)$ is the complex dimension of the $\text{Gr}(2r + 1, 2k)$.

---

[20] If $k < 2$ the index vanishes.

For the second partition $m_*^{(2)} = (m_1 = 2, \, m_2 = 0)$, the type of bipartite graphs $G = (V_L + V_R, E) \in \mathcal{G}(\vec{L}_{m_*^{(2)},r})$ defined in §2.3 has[21]

$$v_L = \sum_\ell m_\ell = 2,$$

$$v_R = Mr + 1 = 2r + 1, \tag{6.20}$$

$$e = Mr + \sum_\ell m_\ell = 2r + 2,$$

where v_L and v_R are the number of vertices in V_L and V_R and e is the total number of edges in G. The 2-dimensional vector is $\vec{L}_{m_*^{(2)},r} = (r, r)$. Each vertex in V_L is incident to $r + 1$ edges. The number of trees in $\mathcal{G}(\vec{L}_{m_*^{(2)},r})$ is given by the tree counting theorem (2.24)

$$T(\vec{L}_{m_*^{(2)},r}) = (2r + 1)\binom{2r}{r}. \tag{6.21}$$

Each tree corresponds to a set of poles with different flavor fugacities ξ that contributes to the index in the residue formula. Due to the Weyl symmetry permuting the N vertices in V_R, each trees contributes the same amount to the index, so it suffices to compute one specific tree and multiply it by $T(\vec{L}_{m_*^{(2)},r})$. For definiteness, let us consider the tree in Figure 20, where the first vertex in V_L is incident to vertices from 1 to r and $2r + 1$ in V_R, while the second vertex in V_L is incident to vertices from $r + 1$ to $2r + 1$ in V_R.

The tree in Figure 20 corresponds to the set of poles specified by

$$u_{2r+1} = \xi_{\mu_0}^{(1)}, \qquad u_1 = \xi_{\mu_1}^{(1)}, \qquad u_2 = \xi_{\mu_2}^{(1)}, \quad \ldots, \qquad u_r = \xi_{\mu_r}^{(1)},$$

$$u_{2r+1} - v = \xi_{\nu_0}^{(2)}, \quad u_{r+1} - v = \xi_{\nu_1}^{(2)}, \quad u_{r+2} - v = \xi_{\nu_2}^{(2)}, \quad \ldots, \quad u_{2r} - v = \xi_{\nu_r}^{(2)}, \tag{6.22}$$

for some $\mu_0, \mu_1, \ldots, \mu_r, \nu_0, \nu_1, \ldots, \nu_r = 1, \ldots, k$. The μ's are all distinct and similarly for ν's. In the end we sum over all such μ's and ν's. Note that the above pole prescription fixes

$$v = \xi_{\mu_0}^{(1)} - \xi_{\nu_0}^{(2)}. \tag{6.23}$$

---

[21] $M = 2$ here.
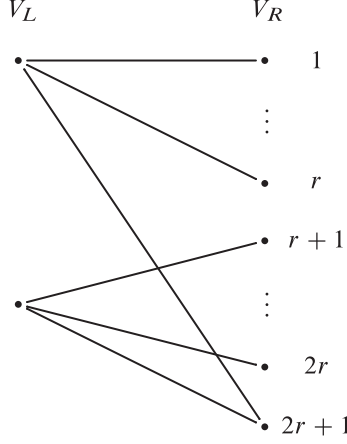
Figure 20. A tree in $\mathcal{G}(\vec{L}_{m_*^{(2)},r})$, where $\vec{L}_{m_*^{(2)},r} = (r,r)$. In this example, $M = 2$ and $m_* = (m_1 = 2, m_2 = 0)$. The first vertex in V_L is incident to vertices from 1 to r and $2r + 1$ in V_R, while the second vertex in V_L is incident to vertices from $r + 1$ to $2r + 1$ in V_R. There are $(2r + 1)\binom{2r}{r}$ such trees, each of which corresponds to a set of poles like (6.22).

The integrand for the Jeffrey–Kirwan residue is given by (4.4)

$$\left(\frac{1}{\sin(z)}\right)^{2r+2} \prod_{\substack{a,b=1 \\ a \neq b}}^{2r+1} \frac{1}{f(u_a - u_b)} \prod_{i=1}^{k} \prod_{a=1}^{2r+1} f(u_a - \xi_i^{(1)}) f(u_a - v - \xi_i^{(2)}), \quad (6.24)$$

where $f(x)$ is defined by (6.10). The arguments of $f(x)$ in the integrand are determined by the position of the pole (6.22). They are

$$u_c - \xi_i^{(1)} = \xi_{\mu_c i}^{(1)}, \qquad\qquad u_{r+c} - \xi_i^{(1)} = \xi_{\mu_0 i}^{(1)} + \xi_{v_c v_0}^{(2)},$$

$$u_c - v - \xi_i^{(2)} = \xi_{\mu_c \mu_0}^{(1)} + \xi_{v_0 i}^{(2)}, \quad u_{r+c} - v - \xi_i^{(2)} = \xi_{v_c i}^{(2)}, \qquad (6.25)$$

$$u_{2r+1} - \xi_i^{(1)} = \xi_{\mu_0 i}^{(1)}, \qquad\qquad u_{2r+1} - \xi_i^{(2)} = \xi_{v_0 i}^{(2)},$$

where $c, d = 1, 2, \ldots, r$ (rather than to $2r + 1$).

Since the refined index does not depend on the flavor fugacities ξ's by the $\mathcal{N} = 4$ supersymmetry, we are again free to evaluate it in the limit (6.13). In this limit $f(x)f(-x) = 1$, so we do not have to consider the factor $\prod_{a \neq b}^{2r+1} \frac{1}{f(u_a - u_b)}$ in the integrand. We can also replace $f(\xi_{\mu_c \mu_0}^{(1)} + \xi_{v_0 i}^{(2)})$ by $f(\xi_{\mu_c \mu_0}^{(1)})$. The index is

then

$$
\Omega(\mathcal{M}^k_{m_*^{(2)},2r+1}, y)
$$

$$
= \frac{1}{r!r!} \sum_{(\mu_0, \mu_1, ..., \mu_r)} \left(\prod_{\substack{i=1 \\ i \neq \mu_0}}^{k} f(\xi^{(1)}_{\mu_0 i})^{r+1} \right) \left(\prod_{c=1}^{r} \prod_{\substack{i=1 \\ i \neq \mu_c}}^{k} f(\xi^{(1)}_{\mu_c i}) \right) \left(\prod_{c=1}^{r} f(\xi^{(1)}_{\mu_c \mu_0})^k \right)
$$

$$
\times \sum_{(\nu_0, \nu_1, ..., \nu_r)} \left(\prod_{\substack{i=1 \\ i \neq \nu_0}}^{k} f(\xi^{(2)}_{\nu_0 i}) \right) \left(\prod_{c=1}^{r} \prod_{\substack{i=1 \\ i \neq \nu_c}}^{k} f(\xi^{(2)}_{\nu_c i}) \right) \left(\prod_{c=1}^{r} f(\xi^{(2)}_{\nu_c \nu_0}) \right),
$$

$$(6.26)$$

where the sum is over all tuples $(\mu_0, \mu_1, \ldots, \mu_r)$ with distinct μ's ranging from 1 to k. Similarly for $(\nu_0, \nu_1, \ldots, \nu_r)$.

Using (6.14), we have

$$
\prod_{\substack{i=1 \\ i \neq \mu_a}}^{k} f(\xi^{(1)}_{\mu_a i}) = y^{k-2\mu_a+1}.
$$

$$(6.27)$$

We can then rewrite the index for the star quiver associated to $m_*^{(2)}$ as

$$
\Omega(\mathcal{M}^k_{m_*^{(2)},2r+1}, y)
$$

$$
= \frac{1}{r!r!} \left(\sum_{(\mu_0, \mu_1, ..., \mu_r)} y^{(2r+1)(k+1)-2(r+1)\mu_0-2\sum_{c=1}^{r}\mu_c - k\sum_{c=1}^{r}\theta(\mu_c-\mu_0)} \right)
$$

$$
\times \left(\sum_{(\nu_0, \nu_1, ..., \nu_r)} y^{(r+1)(k+1)-2\nu_0-2\sum_{c=1}^{r}\nu_c - \sum_{c=1}^{r}\theta(\nu_c-\nu_0)} \right).
$$

$$(6.28)$$

Again the sum is over all tuples $(\mu_0, \mu_1, \ldots, \mu_r)$ with distinct μ's ranging from 1 to k. Similarly for $(\nu_0, \nu_1, \ldots, \nu_r)$, and θ is the step function defined in (6.15).

Assembling the pieces using the degeneration formula (6.3), we arrive at our final expression for the refined index of the Kronecker quiver with dimension vector $(2, 2r + 1)$

$$
\Omega(2, 2r+1, k, y) = y^{-2-d} \Big[-\frac{1}{2(1+y^2)} y^{d_{m_*^{(1)}}} \Omega(\mathcal{M}^k_{m_*^{(1)},2r+1}, y)
$$

$$
+ \frac{1}{2} y^{d_{m_*^{(2)}}} \Omega(\mathcal{M}^k_{m_*^{(2)},2r+1}, y) \Big],
$$

$$(6.29)$$

if $d = (2r+1)(2k-2r-1) - 3 \geq 0$ and zero otherwise. Here

$$
d_{m_*^{(1)}} = (2r+1)(2k-2r-1)
$$

and

$$d_{m_*^{(2)}} = 2k(2r + 1) - (2r + 1)^2 - 1$$

are the ranks of the star quivers associated to the partitions $m_*^{(1)}$ and $m_*^{(2)}$, respectively. $\Omega(\mathcal{M}^k_{m_*^{(1)}, 2r+1}, y)$ is the refined index for the Grassmannian $\mathrm{Gr}(2j + 1, 2k)$ given in (6.19).

We list the first few examples of the refined index $\Omega(M, N, k, y)$ in the following.[22]

$k = 2$:

$$\Omega(2, 1, 2, y) = 1; \tag{6.30a}$$

$k = 3$:

$$\Omega(2, 1, 3, y) = \frac{1}{y^2} + 1 + y^2, \tag{6.30b}$$

$$\Omega(2, 3, 3, y) = \frac{1}{y^6} + \frac{1}{y^4} + \frac{3}{y^2} + 3 + 3y^2 + y^4 + y^6; \tag{6.30c}$$

$k = 4$:

$$\Omega(2, 1, 4, y) = \frac{1}{y^4} + \frac{1}{y^2} + 2 + y^2 + y^4, \tag{6.30d}$$

$$\begin{aligned}
\Omega(2, 3, 4, y) &= \frac{1}{y^{12}} + \frac{1}{y^{10}} + \frac{3}{y^8} + \frac{4}{y^6} + \frac{7}{y^4} + \frac{8}{y^2} \\
&\quad + 10 + 8y^2 + 7y^4 + 4y^6 + 3y^8 + y^{10} + y^{12};
\end{aligned} \tag{6.30e}$$

$k = 5$:

$$\Omega(2, 1, 5, y) = \frac{1}{y^6} + \frac{1}{y^4} + \frac{2}{y^2} + 2 + 2y^2 + y^4 + y^6, \tag{6.30f}$$

$$\begin{aligned}
\Omega(2, 3, 5, y) &= \frac{1}{y^{18}} + \frac{1}{y^{16}} + \frac{3}{y^{14}} + \frac{4}{y^{12}} + \frac{7}{y^{10}} + \frac{9}{y^8} + \frac{14}{y^6} + \frac{16}{y^4} + \frac{20}{y^2} \\
&\quad + 20 + 20y^2 + 16y^4 + 14y^6 + 9y^8 + 7y^{10} + 4y^{12} + 3y^{14} \\
&\quad + y^{16} + y^{18},
\end{aligned} \tag{6.30g}$$

---

[22] For each k, the remaining cases not listed in (6.30) are redundant as a consequence of the isomorphism (3.10) $\Omega(2, 2r + 1, k) = \Omega(2, 2(k - r - 1) + 1, k)$.

$$\Omega(2,5,5,y) = \frac{1}{y^{22}} + \frac{1}{y^{20}} + \frac{3}{y^{18}} + \frac{4}{y^{16}} + \frac{8}{y^{14}} + \frac{11}{y^{12}} + \frac{17}{y^{10}} + \frac{22}{y^8}$$
$$+ \frac{30}{y^6} + \frac{35}{y^4} + \frac{41}{y^2} + 41 + 41y^2 + 35y^4 + 30y^6 + 22y^8 \quad \text{(6.30h)}$$
$$+ 17y^{10} + 11y^{12} + 8y^{14} + 4y^{16} + 3y^{18} + y^{20} + y^{22}.$$

We have checked that the above refined indices agree with [2].

Appendices

A. An identity for $[x^M]\{\exp(\beta F)\}$ when $r = 1$

In this appendix, we provide a direct calculation of the power series coefficients of $\exp[\beta F(k, 1, x)]$ for arbitrary complex β.

We first prove a lemma.[23]

Lemma 2. *Let k and M be positive integers and*

$$F(k,1,x) = \sum_{\ell=1}^{\infty} \frac{(-1)^{\ell-1}}{\ell^2} (\ell+1) \binom{k\ell}{\ell+1} x^{\ell}.$$

Then

$$F(k, 1, y(1+y)^{k-1}) = k(k-1) \log(1+y). \quad \text{(A.1)}$$

---

[23] We thank Noam D. Elkies and Ira Gessel for pointing out this identity to us.

Proof. We will prove this by direct substitution. The lefthand side equals to

$$F(k, 1, y(1 + y)^{k-1})$$

$$= \sum_{\ell=1}^{\infty} \frac{(-1)^{\ell-1}}{\ell^2} (\ell + 1) \binom{k\ell}{\ell + 1} y^{\ell} \times \left[\sum_{s=0}^{\ell(k-1)} \binom{\ell(k - 1)}{s} y^s \right]. \tag{A.2}$$

It follows that

$$[y^n]\{F(k, 1, y(1 + y)^{k-1})\} = \sum_{\ell=1}^{n} \frac{(-1)^{\ell-1}}{\ell^2} (\ell + 1) \binom{k\ell}{\ell + 1} \binom{(k - 1)\ell}{n - \ell}$$

$$= -\frac{k(k - 1)}{n!} \sum_{\ell=1}^{n} (-1)^{\ell} \binom{n}{\ell} \prod_{i=1}^{n-1} (k\ell - i). \tag{A.3}$$

Note that for $m \in \mathbb{N}$,

$$\left(x \frac{d}{dx} \right)^m (1 - x)^n = \sum_{\ell=1}^{n} (-1)^{\ell} \binom{n}{\ell} \ell^m x^n. \tag{A.4}$$

Setting $x = 1$, it follows that

$$\sum_{\ell=1}^{n} (-1)^{\ell} \binom{n}{\ell} \ell^m = 0 \quad \text{if } n > m \geq 1. \tag{A.5}$$

Using the above identity, we see that all the higher order terms in ℓ in (A.3) vanish after summing over ℓ, and we are left with

$$[y^n]\{F(k, 1, y(1 + y)^{k-1})\} = -\frac{k(k - 1)}{n!} \sum_{\ell=1}^{n} (-1)^{\ell} \binom{n}{\ell} \prod_{i=1}^{n-1} (-i)$$

$$= (-1)^{n-1} \frac{k(k - 1)}{n}. \tag{A.6}$$

This concludes the proof of the lemma. $\qquad\qquad\qquad\qquad\qquad\qquad\square$

Theorem 3. *Let k and M be positive integers and*

$$F(k, 1, x) = \sum_{\ell=1}^{\infty} \frac{(-1)^{\ell-1}}{\ell^2}(\ell + 1)\binom{k\ell}{\ell+1}x^{\ell}.$$

Let β be a complex number. Then

$$[x^M]\{\exp[\beta F(k, 1, x)]\} = \frac{\beta}{M}k(k-1)\binom{k(k-1)\beta - (k-1)M - 1}{M-1}. \quad (A.7)$$

Proof. From Lemma 2, we have

$$\exp[\beta F(k, 1, x)] = (1 + y(x))^{\beta k(k-1)} = \sum_{\ell=0}^{\infty} \binom{\beta k(k-1)}{\ell} y(x)^{\ell}, \quad (A.8)$$

where $y(x)$ is defined as the solution to

$$x = y(1 + y)^{k-1}. \quad (A.9)$$

The Taylor series coefficient of $y(x)^{\ell}$ can be obtained by the Lagrange inversion theorem (see, for example, [47, 48]),

$$y(x)^{\ell} = \sum_{m=0}^{\infty} (-1)^m \frac{\ell}{m+\ell}\binom{(k-1)(m+\ell) + m - 1}{m}x^{m+\ell}. \quad (A.10)$$

Plugging this into (A.8), we have

$$[x^M]\{\exp[\beta F(k, 1, x)]\} = \frac{1}{M}\sum_{\ell=1}^{M}(-1)^{M-\ell}\ell\binom{\beta k(k-1)}{\ell}\binom{kM - \ell - 1}{M - \ell}. \quad (A.11)$$

Note that right-hand-sides of both (A.7) and (A.11) are polynomials in β of degree M. To show that they are the same, it suffices to show that they have the same roots in β, while the overall constant can be trivially checked by plugging some specific values of M, β, k. Due to the binomial coefficient, (A.7) has zeroes at $\beta = 0$ and

$$\beta = \frac{1}{k(k-1)}(kM - s), \quad s = 1, \ldots, M - 1. \quad (A.12)$$

Obviously (A.11) vanishes when $\beta = 0$. It remains to show that (A.11) vanishes when β takes value in (A.12). When $k(k-1)\beta = (k-1)M - s$, (A.11) can be written as

$$
\frac{(-1)^M}{M \times M!} \sum_{\ell=1}^{M} (-1)^\ell \ell \binom{M}{\ell} \frac{(kM-s)!}{(kM-(\ell+s))!} \frac{(kM-(\ell+1))!}{(kM-M-1)!}
$$

$$
= \frac{(-1)^M}{M \times M!} \frac{(kM-s)!}{(kM-M-1)!} \tag{A.13}
$$

$$
\sum_{\ell=1}^{M} (-1)^\ell \binom{M}{\ell} \ell (kM-(\ell+1))\ldots(kM-(\ell+s-1)).
$$

Note $\ell(kM-(\ell+1))\ldots(kM-(\ell+s))$ is a polynomial in ℓ of degree s. Since $s < M$, it follows from (A.5) that (A.13) is zero. Thus we have shown that $\beta = \frac{1}{k(k-1)}(kM - s)$ with $s = 1,\ldots,M-1$ and $\beta = 0$ are roots for (A.11), which are the same M roots of (A.7). This completes the proof. □

B. Degenerate poles

In §4 we have computed the contributions to the index from the non-degenerate poles in the residue formula (4.2). Here, we conjecture that the degenerate poles do not contribute when $N = Mr + 1$.

Let us give evidence motivating our claim. Consider an integrand of the form

$$
\frac{\sin[A^{(1)}(u)]\ldots\sin[A^{(q)}(u)]}{\sin[B^{(1)}(u)]\ldots\sin[B^{(p)}(u)]} \ldots, \tag{B.1}
$$

where $A^{(i)}(u)$ and $B^{(i)}(u)$ are some linear functions of the gauge fugacities[24] u_α. The ... represents terms that are nonzero and finite at the pole. The index α runs over $1,\ldots,e$, where e is the total rank of the gauge group. Suppose at a point $u = u_*$, we have

$$
A^{(i)}(u_*) = 0, \quad B^{(i)}(u_*) = 0. \tag{B.2}
$$

Then $u = u_*$ is called a degenerate pole if $p > e$, and a non-degenerate pole if $p = e$ and $q = 0$. For the degenerate poles in the star quiver, we always

[24] As an abuse of notations, in the general discussion here we use u_α to represent both the gauge fugacities of the non-abelian node u_a and of the abelian nodes $v_I^{(\ell)}$ in the star quiver (Figure 7).

have $p - q = e$, so they are effectively simple poles after carefully "canceling" the zeroes in the numerator and the denominator. We will be precise about this cancellation in a moment.

Let u_* be a degenerate pole with $p - q = e$. As far as the residue at $u = u_*$ is concerned, we can replace $\sin\left[A^{(i)}(u)\right]$ and $\sin\left[B^{(i)}(u)\right]$ by their arguments.[25] After doing so, we perform partial fraction decomposition to break (B.1) into simple poles:

$$\frac{A^{(1)}(u)\dots A^{(q)}(u)}{B^{(1)}(u)\dots B^{(p)}(u)} = \sum_w \frac{1}{C^{(1,w)}(u)\dots C^{(e,w)}(u)}, \qquad \text{(B.3)}$$

for some linear functions $C^{(a,w)}(u)$ of u_α. Now the terms on the righthand side become non-degenerate poles and we can evaluate their residue at $u = u_*$ using the technique in §4.2. In other words, *we have decomposed a degenerate pole with $p - q = e$ into a sum of non-degenerate poles.*

In the star quiver $\mathcal{M}^k_{m_*,N}$ with $N = Mr + 1$, the degenerate poles decompose into non-degenerate poles as described above. We claim that none of these non-degenerate poles satisfies the Jeffrey–Kirwan rule of §4.2 and therefore they do not contribute to the index.

Let us demonstrate this claim in an explicit example. Let $M = 3$, $r = 1$, $e = 6$, and $m_* = (m_1 = 3, m_2 = 0, m_3 = 0)$. An example of a degenerate pole is[26]

$$
\begin{aligned}
u_1 - v_1 - \xi_1^{(1)} &= 0, \quad u_2 - v_1 - \xi_1^{(1)} = 0, \\
u_1 - v_2 - \xi_1^{(2)} &= 0, \quad u_2 - v_2 - \xi_1^{(2)} = 0, \quad u_3 - v_2 - \xi_2^{(2)} = 0, \\
u_1 - v_3 - \xi_1^{(3)} &= 0, \quad u_2 - v_3 - \xi_1^{(3)} = 0, \quad u_4 - v_3 - \xi_2^{(3)} = 0.
\end{aligned}
\qquad \text{(B.4)}
$$

These correspond to the $p = 8$ sine factors that vanish at $u = u_*$ in the denominator of (B.1). Note that since $u_1 - v_2 - \xi_1^{(2)} = 0$ and $u_2 - v_2 - \xi_1^{(2)} = 0$, we have $u_1 = u_2$ at this pole. This results in $q = 2$ sine factors that vanish at $u = u_*$ in the numerator of (B.1),

$$\sin(u_1 - u_2)\sin(u_2 - u_1). \qquad \text{(B.5)}$$

Note that indeed we have $p - q = e$.

---

[25] It is not, however, legitimate to replace the sine factors in $\dots$ of (B.1) by their arguments as they do not vanish at u_*.

[26] For simplicity of notation, we will denote $v_I^{\ell=1}$ simply by v_I as there are no other values of ℓ for the partition $m_* = (m_1 = 3, m_2 = 0, m_3 = 0)$. We also abbreviate $\xi_i^{(I,\ell=1)}$ by $\xi_i^{(I)}$. As usual $v_1 = v_1^{(1)}$ is understood to be zero since it corresponds to the decoupled abelian node.

Now performing the partial fraction decomposition, there are four terms on the righthand side of (B.3), each of which corresponds to a non-degenerate pole. For example, one of them is

$$
\begin{aligned}
&u_1 - v_1 - \xi_1^{(1)} = 0, \\
&u_1 - v_2 - \xi_1^{(2)} = 0, \quad u_3 - v_2 - \xi_2^{(2)} = 0, \\
&u_1 - v_3 - \xi_1^{(3)} = 0, \quad u_2 - v_3 - \xi_1^{(3)} = 0, \quad u_4 - v_3 - \xi_2^{(3)} = 0.
\end{aligned}
\tag{B.6}
$$

However, this non-degenerate pole does not satisfy the Jeffrey–Kirwan rule. For example, there should be $\ell r + 1 = 2$ sine factors with arguments $u_a - v_1 - \xi$, whereas there is only one above. It follows that this non-degenerate pole does not contribute to the index. Similarly one can show the other three non-degenerate poles also violate the Jeffrey–Kirwan rule. Hence the degenerate pole (B.4), which equals to the sum of four non-degenerate poles, does not contribute to the index.

More generally we conjecture that degenerate poles do not contribute to the index when $N = Mr + 1$. The fact that our final expressions match with results produced by the wall-crossing formula in Section 3.3 gives strong evidence for this claim. Nevertheless, it would be useful to provide an exact proof along the lines suggested above since such a proof is likely to point to other dimension vectors (M, N) amenable to analysis.

References

[1] F. Denef, Quantum quivers and Hall / hole halos. *J. High Energy Phys.* **2002**, no. 10, 023. MR 1952307

[2] M. Reineke, The Harder–Narasimhan system in quantum groups and cohomology of quiver moduli. *Invent. Math.* **152** (2003), no. 2, 349–368. MR 1974891 Zbl 1043.17010

[3] M. Kontsevich and Y. Soibelman, Stability structures, motivic Donaldson–Thomas invariants and cluster transformations. Preprint 2011. arXiv:0811.2435 [math.AG]

[4] M. Gross and R. Pandharipande, Quivers, curves, and the tropical vertex. *Port. Math.* **67** (2010), no. 2, 211–259. MR 2662867 Zbl 227.14049

[5] M. Reineke, Cohomology of quiver moduli, functional equations, and integrality of Donaldson–Thomas type invariants. *Compos. Math.* **147** (2011), no. 3, 943–964. MR 2801406 Zbl 1266.16013

[6] D. Galakhov, P. Longhi, T. Mainiero, G. W. Moore, and A. Neitzke, Wild wall crossing and BPS giants. *J. High Energy Phys.* **1311** (2013), 046.

[7] D. Galakhov, P. Longhi, and G. W. Moore, *Comm. Math. Phys.* **340** (2015), no. 1, 171–232. MR 3395151 Zbl 1344.81141

[8] T. Weist, Localization in quiver moduli spaces. *Represent. Theory* **17** (2013), 382–425.
MR 3073549 Zbl 1302.14010

[9] T. Weist, On the Euler characteristic of Kronecker moduli spaces. *J. Algebraic Combin.* **38** (2013), no. 3, 567–583. MR 3104729 Zbl 1278.14014

[10] C. Hwang, J. Kim, S. Kim, and J. Park, General instanton counting and 5d SCFT. *J. High Energy Phys.* **2015**, no. 7, 063. MR 3384152

[11] C. Córdova and S.-H. Shao, An index formula for supersymmetric quantum mechanics. *J. Singul.* **15** (2016), 14–35. MR 3562853 Zbl 1346.81120

[12] K. Hori, H. Kim, and P. Yi, Witten index and wall crossing. *J. High Energy Phys.* **2015**, no. 1, 124. MR 3313918

[13] L. C. Jeffrey and F. C. Kirwan, Localization for nonabelian group actions. *Topology* **34** (1995), no. 2, 291–327. MR 1318878 Zbl 0833.55009

[14] M. R. Douglas, B. Fiol, and C. Romelsberger, Stability and BPS branes. *J. High Energy Phys.* **2005**, no. 9, 006. MR 2171358

[15] M. R. Douglas, B. Fiol, and C. Romelsberger, The Spectrum of BPS branes on a noncompact Calabi–Yau. *J. High Energy Phys.* **2005**, no. 9, 057. MR 2174156

[16] B. Fiol and M. Marino, BPS states and algebras from quivers. *J. High Energy Phys.* **2000**, no. 7, 031. MR 1780370 Zbl 0965.81067

[17] B. Fiol, The BPS spectrum of $\mathcal{N} = 2\,\mathrm{SU}(N)$ SYM. *J. High Energy Phys.* **2006**, no. 2, 065. MR 2219440

[18] F. Denef and G. W. Moore, Split states, entropy enigmas, holes and halos. *J. High Energy Phys.* **2011**, no. 11, 129. MR 2913216 Zbl 1306.81213

[19] M. Alim, S. Cecotti, C. Córdova, S. Espahbodi, A. Rastogi, et al., $\mathcal{N} = 2$ quantum field theories and their BPS quivers. *Adv. Theor. Math. Phys.* **18** (2014), no. 1, 27–127. MR 3268234 Zbl 1309.81142

[20] J. Manschot, B. Pioline, and A. Sen, From black holes to quivers. *J. High Energy Phys.* **2012**, no. 11, 023. MR 3036499

[21] S. Cecotti and M. Del Zotto, Half-hypers and quivers. *J. High Energy Phys.* **2012**, no. 9, 135. MR 3044914

[22] W.-y. Chuang, D.-E. Diaconescu, J. Manschot, G. W. Moore, and Y. Soibelman, Geometric engineering of (framed) BPS states. *Adv. Theor. Math. Phys.* **18** (2014), no. 5, 1063–1231. MR 3281276 Zbl 1365.81092

[23] C. Córdova and A. Neitzke, Line defects, tropicalization, and multi-centered quiver quantum mechanics. *J. High Energy Phys.* **2014**, no. 9, 099. MR 326798 Zbl 1333.81166

[24] C. Córdova, Regge trajectories in $\mathcal{N} = 2$ supersymmetric Yang–Mills theory. *J. High Energy Phys.* **2016**, no. 9, 020. MR 3557923

[25] C. Córdova and S.-H. Shao, Asymptotics of ground state degeneracies in quiver quantum mechanics. *Commun. Number Theory Phys.* **10** (2016), no. 2, 339–371. MR 3528836 Zbl 1346.81067

[26] T. Mainiero, Algebraicity and asymptotics: an explosion of BPS indices from algebraic generating series. Preprint 2016. arXiv:1606.02693 [hep-th]

[27] P. C. Argyres and M. R. Douglas, New phenomena in SU(3) supersymmetric gauge theory. *Nuclear Phys.* B **448** (1995), no. 1-2, 93–126. MR 1352402 Zbl 1009.81572

[28] D. Gaiotto, G. W. Moore, and A. Neitzke, Wall-crossing, Hitchin systems, and the WKB approximation. *Adv. Math.* **234** (2013), 239–403. MR 3003931 Zbl 1358.81150

[29] M. Alim, S. Cecotti, C. Córdova, S. Espahbodi, A. Rastogi, and C. Vafa, BPS quivers and spectra of complete $\mathcal{N} = 2$ quantum field theories. *Comm. Math. Phys.* **323** (2013), no. 3, 1185–1227. MR 3106506 Zbl 1305.81118

[30] N. Seiberg and E. Witten, Electric–magnetic duality, monopole condensation, and confinement in $N = 2$ supersymmetric Yang–Mills theory. *Nuclear Phys. B* **426** (1994), no. 1, 19–52. MR 1293681 Zbl 0996.81510

[31] R. Gopakumar and C. Vafa, M theory and topological strings–I. arXiv:hep-th/9809187 [hep-th]

[32] R. Gopakumar and C. Vafa, M theory and topological strings–II. arXiv:hep-th/9812127 [hep-th]

[33] F. Denef, Supergravity flows and D-brane stability. *J. High Energy Phys.* **2000**, no. 8, 050. MR 1792870 Zbl 0990.83553

[34] F. Denef, On the correspondence between D-branes and stationary supergravity solutions of type II Calabi–Yau compactifications. In E. D'Hoker, D. Phong and S.-T. Yau (eds.), *Mirror symmetry*. IV. Proceedings of the Conference on Strings, Duality, and Geometry held at the University of Montreal, Montreal, QC, March 2000. AMS/IP Studies in Advanced Mathematics, 33. American Mathematical Society, Providence, R.I., and International Press, Somerville, MA, 2002, 209–230. MR 1969028 Zbl 1067.83016

[35] A. D. King, Moduli of representations of finite dimensional algebras. *Quart. J. Math. Oxford Ser.* (2) **45** (1994), no. 180, 515–530. MR 1315461 Zbl 0837.16005

[36] P. Gabriel, Unzerlegbare Darstellungen. I. *Manuscripta Math.* **6** (1972), 71–103; correction, ibid. **6** (1972), 309. MR 0332887 Zbl 0232.08001

[37] I. N. Bernšteĭn, I. M. Gel′fand, and V. A. Ponomarev, Coxeter functors and Gabriel's theorem. *Uspehi Mat. Nauk* **28** (1973), no. 2(170), 19–33. In Russian. English translation, *Russian Math. Surveys* **28** (1973), no. 2, 17–32. MR 0393065 Zbl 0269.08001 Zbl 0279.08001 (transl.)

[38] D. Gaiotto, G. W. Moore, and A. Neitzke, Framed BPS states. *Adv. Theor. Math. Phys.* **17** (2013), no. 2, 241–397. MR 3250763 Zbl 1290.81146

[39] M. Del Zotto and A. Sen, About the absence of exotics and the Coulomb branch formula. Preprint 2014. arXiv:1409.5442 [hep-th]

[40] J. Manschot, B. Pioline, and A. Sen, Wall crossing from Boltzmann black hole halos. *J. High Energy Phys.* **2011**, no. 7, 059. MR 2875965 Zbl 1298.81320

[41] M. Reineke, J. Stoppa, and T. Weist, MPS degeneration formula for quiver moduli and refined GW/Kronecker correspondence. *Geom. Topol.* **16** (2012), no. 4, 2097–2134. MR 3033514 Zbl 1276.14085

[42] R. Stanley, *Enumerative combinatorics.* Vol. II. Cambridge Studies in Advanced Mathematics. 62. Cambridge University Press, Cambridge, 2001. Zbl 0978.05002

[43] R. L. Graham, D. E. Knuth, and O. Patashnik, *Concrete mathematics.* A Foundation for Computer Science. Second edition. Addison-Wesley Publishing Company, Reading, MA, 1994. MR 1397498 Zbl 0836.00001

[44] F. Benini, R. Eager, K. Hori, and Y. Tachikawa, Elliptic genera of two-dimensional $\mathcal{N} = 2$ gauge theories with rank-one gauge groups. *Lett. Math. Phys.* **104** (2014), no. 4, 465–493. MR 3177993 Zbl 1312.58008

[45] F. Benini, R. Eager, K. Hori, and Y. Tachikawa, Elliptic genera of 2d $\mathcal{N} = 2$ gauge theories. *Comm. Math. Phys.* **333** (2015), no. 3, 1241–1286. MR 3302634 Zbl 1321.81059

[46] R. Gould, *Graph theory.* Corrected reprint of the 1988 original. Dover Publications, Mineola, N.Y., 2012. MR 3114560 Zbl 1284.05003

[47] N. D. Elkies, The power series for the inverse function of $y(1 − y)^t$. http://www.math.harvard.edu/~elkies/Misc/catalan.pdf

[48] N. D. Elkies, Yet another proof of the series in x for the powers y^β of the solution of $y(1 − y)^t = x$. http://www.math.harvard.edu/~elkies/Misc/catalan2.pdf

Clay Córdova, Society of Fellows, Harvard University,
78 Mount Auburn Street, Cambridge, MA 02138, USA

e-mail: cordova@physics.harvard.edu

Shu-Heng Shao, Jefferson Physical Laboratory, Harvard University, Cambridge,
MA 02138, USA

e-mail: shshao@physics.harvard.edu